REPORT DOCUMENTATION PAGE

Form Approved OMB NO. 0704-0188

1. REPORT DATE (DD-MM-YYYY)	2. REPORT TYPE	3. DATES COVERED (From - To)
06-07-2022	Final Report	1-Oct-2018 - 30-Jun-2020

4. TITLE AND SUBTITLE

Final Report: Synthesis and characterization of graphitic shell coated metal nanoparticles: A facile design to preserve and enhance interfacial activities of energetic nanomaterials.

5a. CONTRACT NUMBER
W911NF-18-2-0305

5b. GRANT NUMBER

5c. PROGRAM ELEMENT NUMBER
611102

6. AUTHORS

5d. PROJECT NUMBER

5e. TASK NUMBER

5f. WORK UNIT NUMBER

7. PERFORMING ORGANIZATION NAMES AND ADDRESSES

University of Tennessee at Knoxville
Office of Sponsored Programs
1534 White Avenue
Knoxville, TN 37996 -1529

8. PERFORMING ORGANIZATION REPORT NUMBER

9. SPONSORING/MONITORING AGENCY NAME(S) AND ADDRESS (ES)

U.S. Army Research Office
P.O. Box 12211
Research Triangle Park, NC 27709-2211

10. SPONSOR/MONITOR'S ACRONYM(S)
ARO

11. SPONSOR/MONITOR'S REPORT NUMBER(S)
73512-CH-II.5

12. DISTRIBUTION AVAILIBILITY STATEMENT

Approved for public release; distribution is unlimited.

13. SUPPLEMENTARY NOTES

The views, opinions and/or findings contained in this report are those of the author(s) and should not contrued as an official Department of the Army position, policy or decision, unless so designated by other documentation.

14. ABSTRACT

15. SUBJECT TERMS

16. SECURITY CLASSIFICATION OF:			17. LIMITATION OF ABSTRACT	15. NUMBER OF PAGES	19a. NAME OF RESPONSIBLE PERSON
a. REPORT	b. ABSTRACT	c. THIS PAGE			Dibyendu Mukherjee
UU	UU	UU	UU		19b. TELEPHONE NUMBER 865-974-2696

RPPR Final Report
as of 12-Jul-2022

Agency Code: 21XD

Proposal Number: 73512CHII **Agreement Number: W911NF-18-2-0305**
INVESTIGATOR(S):

Name: Dibyendu Mukherjee
Email: dmukherj@utk.edu
Phone Number: 8659742696
Principal: Y

Organization: **University of Tennessee at Knoxville**
Address: Office of Sponsored Programs, Knoxville, TN 379961529
Country: USA
DUNS Number: 003387891 EIN: 626001636
Report Date: 30-Sep-2020 Date Received: 06-Jul-2022
Final Report for Period Beginning 01-Oct-2018 and Ending 30-Jun-2020
Title: Synthesis and characterization of graphitic shell coated metal nanoparticles: A facile design to preserve and enhance interfacial activities of energetic nanomaterials.
Begin Performance Period: 01-Oct-2018 **End Performance Period:** 30-Jun-2020
Report Term: 0-Other
Submitted By: Dibyendu Mukherjee Email: dmukherj@utk.edu
Phone: (865) 974-2696
Distribution Statement: 1-Approved for public release; distribution is unlimited.

STEM Degrees: 2 **STEM Participants:** 2

Major Goals: 1.1. Conspectus - -
Energetic nanomaterials is prominent in solid-state propellants, explosives and pyrotechnics due to the anticipated enhanced oxidation kinetics and ignition in nanoscale regimes. This is largely attributed to their high specific surface areas, metastable structures and smaller diffusion lengths at fuel-oxidizer interfaces. Past works have investigated energetic properties of various metal Nano-Particles, NPs, Al, Ni, Si, etc.[1-3] Enhanced burning rates and ignition of composite Al powder/oxidizer mixtures had peaked past research efforts.[4-8] This includes the PIs' work towards use of Nano-Al in explosives and pyrotechnics [9-11] that have improved our fundamental understanding of their size-dependent properties and heat release mechanisms at nano-scale.[6-8,11-14] Yet, the large heat release in these first-generation energetic nanomaterials have been offset by relatively hindered detonation rates due to the solid-state fuel-oxidizer diffusion lengths and rates being limited by the excessive surface oxide shell formations[11] and NP aggregations. To this end, a few recent research efforts have focused on energetic behaviors arising from surface structural scaffoldings, onion-like layers or nanocages, that lead to excess internal stresses within the solid metal NP cores and promote enhanced energetic behaviors along with other inorganic fullerene-like shell-core nanostructures.[15,16] Yet, there exists a weak fundamental understanding and considerable challenges in the rational design and synthesis of these designer nano-architectures to tap into their potential as future energetic materials. Past works have shown that particle size and morphology, phase changes including surface oxide layer thicknesses can significantly affect the energetic properties of Al NPs.[11,17] In this sense, increasing efforts have been directed towards suitable coating of metal NP surfaces to promote safety, and stymie the surface oxidation without retarding their activities to achieve optimal performance in next-generation energetic nanomaterials. Specifically, carbon coatings have been employed on Al NPs [18] that provide the added advantage that while the coating itself oxidizes into gaseous products, such as CO2, CO etc., to prevent any solid ash residues on the particle surface during its burning, the presence of carbon shell also retards NP aggregation. But the challenge here remains in synthesizing these encapsulated NPs via facile, robust and yet, chemically clean pathways that does not contaminate and/or oxidize the solid fuel cores.

1.2. Critical Bottleneck --
The critical bottleneck exists in the robust synthesis and structural characterizations of next-generation metastable nanomaterials whose surface reactivity can be tuned via structural re-arrangement of surface atoms in NPs [<10 nm sizes]. Such basic science knowledge will also advance the design of Structural Bond Energy Release, SBER, materials, wherein core NPs can be encapsulated in fullerene-like shells under exceedingly high pressure and excessive internal stress, thereby allowing their release, surface reaction rates and hence, energetic behavior to be kinetically controlled.

1.3. Objectives --
We address the aforementioned basic science question with rational design, synthesis and structure-property characterizations of metastable nanostructures with fullerene-like, onion layered/graphitic surface nanocages encapsulating energetic metal NP (Al, Ni, Zr) cores, Fig. 1 in uploads. Such nanomaterials will allow tailored reconstruction of surface structures that can lead to rate-controlled release of combustible solid propellants under high pressure [~10-20 GPa]/temperature to prevent oxide shell-mediated surface passivation. A fundamental understanding of synthesis-structure-property relations in such shell-core nanostructured materials will pave the path for next-generation energetic materials whose surface reactivity and energy release rates are not diffusion-limited.

1.4. Proposed Scientific Approach --
The aforementioned nanostructures will be synthesized via tandem laser ablation synthesis in solution-galvanic replacement reactions, LASiS-GRR [Patent Nos: US 10,326,146 B2 (2019); US 11,127,956 B2 202)] [19-24] - a one-step, one-pot, 'green' synthesis route recently patented by the PI's group that brings in a disruptive merger of high-energy driven non-equilibrium 'top-down' LASiS with chemical kinetics driven 'bottom-up' GRR to tailor-make complex multi-elemental metastable nanostructures heretofore inconceivable via equilibrium synthesis routes. The transformative concept is that seeding NPs from rate-limiting LASiS drive redox chemistry in rate-controlling GRR to initiate highly non-equilibrium nucleation pathways at the laser-induced plasma-liquid interface. In turn, it facilitates the production of NPs with metastable heterostructures and tailored sizes/shapes, compositions without using any external surfactants, ligands, etc.

Our central hypothesis is that the non-equilibrium thermodynamics and kinetics of high-energy LASiS-GRR technique can be tuned by laser, solvent, high-energy plasma and redox driven process parameters to tailor sizes/shapes, metastable interfacial structures/scaffoldings, architectures, and compositions of graphitic/fullerene shell coated heteronanostructured materials with energetic/pyrophoric structure-property relations.

The fundamental technique behind the proposed tandem LASiS-GRR route involves the thermal vaporization of organic solvent-confined metal targets with high-energy laser [Nd:YAG pulsed laser;wavelength= 1064 nm; pulse energies ~165, 330 mJ/pulse] inside a reactor cell with inert gas atmosphere. This generates a micro plasma with excess temperatures [~4000-5000 K] and pressures [~10-15 GPa] that thermally vaporizes the target material to nucleate seeding metal NPs inside the plasma-induced cavitation bubble. The seeding NPs undergo ultrafast collisional quenching and chemical reactions along with solvent pyrolysis at the bubble-liquid interface, Fig. 2 in uploads. Here the scientific rationale is that the thermodynamics of heterogeneous composites and phase formations, although rate-limited by the nucleation of seeding NPs from LASiS, is finally controlled by the rate kinetics of the chemical reactions initiated at the cavitation bubble/solvent interface.[20] Finally, secondary metals from the chemical reactions and/or, graphitic carbon from the solvent pyrolysis undergo heterogeneous nucleation on the seeding NP surface sites.

Proposed LASiS-GRR technique allows simultaneous tailoring of: 1 - sizes/shapes, crystallinity by tuning laser parameters [fluence, wavelength]; and 2 - composition, alloying/composite formation, and morphology by tuning solvent chemistry, type of solvent, pH, precursor salt concentrations, temperature, sonication. Process parameters to control the LASiS technique are:[19-22] 1 - Laser wavelengths [1064 and 532 nm] and energies [~70-330 mJ/pulse]; 2 - Solution pH; 3 - Metal targets and precursors with optimal redox potentials to control NP shape/structure; 4 - Choice of aqueous, organic or cryogenic solvents to tailor desired interfacial structurers, onion-like multilayers of graphitic shells. Specifically, we hypothesize that high vapor pressure organic solvents can promote the formation of metastable interfacial structures with fullerene-like interlayers due to the generation of liquid-confined high-pressure conditions.

1.5. Broader Technological Impacts on Army Mission --
Technological impacts will expedite the development of advanced nanomanufacturing processes based on the engineering know-how garnered from the LASiS-GRR technique. Such developments can provide fresh paradigms in the rapid discovery and deployment of new classes of composite metastable nanomaterials that can find home in diverse defense applications as solid-state propellants and explosives.

Accomplishments: 1. Abstract -
We report final results for Contract No.: W911NF1820305 on - synthesis of graphitic shell coated Al NPs [less than 20 nm] via Laser Ablation Synthesis in solution, LASiS, to preserve high surface areas and interfacial properties of Al NPs [Published article: S. A. Davari, et al. Appl. Surf. Sci., 473, 156 - 2019 is uploaded for detailed results]. Herein, we use a high-energy laser to ablate Al pellets confined in either acetone or toluene to coat active Al NP core with graphitic shells generated from thermal pyrolysis of the organic solvents. Energetic activities of the C/Al NPs were tested via Laser-induced Air Shock from Energetic Materials, LASEM, technique. We demonstrated that

synthesis parameters such as organic solvents, laser flux and ablation times can be tuned to tailor NP sizes/aggregation with the aid of the C shell formations and, in turn, their energetic behavior. This study unveils the synthesis-structure-property relations in LASiS-based manufacturing of energetic nanocapsules within graphitic shells that are safe to handle and can undergo kinetically controlled spontaneous energy release under desired conditions.

2. Experimental activities -
2.1. Synthesis of Al NPs -
Al targets [99.99% purity] mounted on a stepper motor were placed in 8 ml of the organic solvents [acetone, 99.95% purity and toluene, 99.9% purity] at room temperature and ablated with a Q-switched Nd-YAG pulsed laser operating at 1064 nm with 4 ns pulse width, 10 Hz repetition rate and maximum energy 330 mJ/pulse [Fig. 3]. Following ablation, NP suspensions were centrifuged, decanted and washed with methanol and finally, the dried powders were stored under inert atmosphere for all the characterization purposes. Commercial Al NPs [80 nm] were purchased from NovaCentrix for all comparison studies.

2.2. Laser-induced Air Shock from Energetic Materials, LASEM -
Energetic tests were carried out via LASEM techniques developed by scientists at the US Army Research Lab [ARL], Aberdeen. LASEM uses high-speed Schlieren imaging to track the expansion of the laser-induced shock wave generated by the plasma from a Nd:YAG laser pulse [1064 nm, 6-ns, 850 mJ] focused on to the sample surface; the measured velocity of the shock wave is indicative of the extent of the energy release on the microsecond timescale. LASEM has been used by ARL teams to estimate the energetic properties of exothermic and explosive materials. For conventional military explosives, strong correlations between characteristic laser-induced shock velocities from the active material and measured detonation velocities from large-scale testing has been reported.[25-27]

3. Significant results and major findings -
LASiS-based synthesis of composite shell-core C/Al NPs in C matrix employed laser ablation on Al pellets for 2-8 mins under either acetone or toluene using laser fluences between 2.6-10.5 J/cm^2. Our results indicate that the size distributions and energetic behavior of the C/Al NPs could be tailored by tuning the organic solvents, laser flux and ablation times. STEM and EELS measurements revealed the size distribution and morphology of the composite C/Al NPs, including the graphitic shell coatings on the Al NP cores [Fig. 4]. Specifically, EELS elemental mapping and HRTEM images for the C/Al NPs synthesized under Acetone indicated that metallic Al cores [10-12 nm] were covered with about 2-3 nm graphitic shell coating [Fig. 6]. Ablation under both Acetone and Toluene generated lognormal Particle Size Distributions [PSD] for C/Al NPs [Fig. 7]. Samples synthesized in acetone showed unimodal distribution with the peak value at 15.7 nm [std. deviation, S.D = 11.0 nm], while those under toluene indicated a bimodal distribution with a major peak at 25 nm [S.D.=25.3 nm] and a minor one at 77.2 nm [S. D.=17.2 nm]. These results were explained in relation to the higher vapor pressure, V.P., for acetone than toluene which, in turn, controlled the nucleation and growth of the C/Al shell-core NPs due to enhanced solvent pyrolysis leading to larger C production under acetone. Effect of ablation time [2-8 mins] indicated that longer ablation times increased the solvent temperature which, in turn, promoted NP aggregation and sintering [Fig. 8]. Effect of laser fluence [2.6 -10.5 J/cm^2] on the PSD indicated decreasing NP modal sizes and spread of the distribution, S.D., with increasing laser fluence [Fig. 9]. This was explained by increased nucleation of primary Al NPs as result of higher saturation ratio from increased Al monomer concentrations under higher laser fluences. Raman spectra for samples prepared in acetone and toluene indicated both the D [defect] and G [graphitic] bands suggesting the presence of amorphous carbon from the pyrolyzed C matrix and the graphitic structures from the C shells respectively in both samples [Fig. 5].
Energetic activities - tested and compared to commercial nano-Al powders [80 nm] using LASEM techniques at ARL, Aberdeen facilities - measured laser-induced shock velocities [m/s] from the C/Al samples and compared them to blank substrates [controls] [Fig. 10, 11]. The results indicated higher energetic activities (increased shock velocities) for samples prepared in acetone or toluene as compared to commercial Al NPs owing to their smaller sizes and the protective graphitic shell coatings on the Al NPs that promoted fast exothermic reactions on the microsecond timescale between active core Al and oxygen, either from the sample or air entrained in the plasma. Specifically, C/Al NPs prepared in acetone exhibited higher shock velocities as compared to the toluene samples, with the samples made from ablation under a laser fluence of 2.6 J/cm2 [peak sizes~15-16 nm with S.D.<11-12] indicating the highest shock velocities [about 755 m/s]. The mechanistic picture behind the energetic activities for LASiS-synthesized C/Al NPs with the highest LASEM activity was studied using thermo-gravimetric analysis, TGA [Fig. 12]. Thermal decomposition of the sample in air as a function of temperature [deg C] indicated an initial decrease in sample weight [% wt.] up to 470 deg C due to the burning of amorphous C-matrices/shells into gaseous CO/CO2. This was followed by solid to molten phase change for Al core prior to the onset of Al oxidation

between 470-700 deg C, where the weight did not change drastically. Beyond 700 deg C, sample % wt. increased dramatically due to the plausible violent rupture of the graphitic shells followed by instant oxidation of the molten Al dispersed from the core NPs. Due to excessive Laplace pressure [10-20 GPa] inside such ultra-small NPs and the drastic lowering of NP melting points, we posit that the high stress-induced rupture of the graphitic C shell plausibly initiates the well-known melt dispersion mechanism or nanoexplosions, wherein active and hot molten Al is released to the oxidizing environment resulting in instantaneous burning/oxidation.

4. Key outcomes and future goals -
The key observations [Fig. 11] are that while the C/Al NPs made via LASiS in toluene behave as exothermic materials when compared to their counterparts grown in acetone that exhibit more explosive properties [i.e., react more rapidly], a definitive conclusion on their exothermic/explosive behaviors would demand further investigation into their structure-property characteristics and reaction propagation mechanisms. In addition, refinement of the synthesis process to produce more homogeneously distributed Al NPs with C shells is part of our ongoing research efforts that could provide additional enhancements in the microsecond-timescale energy release. In summary, our work here paves the path for the future design of energetic metal/intermetallic NPs encapsulated in nanostructured graphitic shell coatings and/or fullerene-like layers that can be tailored via LASiS-based techniques to tune their reactive behaviors for a myriad of defense and solid-state propellant applications.

Training Opportunities: The current ARO-STIR grant award Contract No.: W911NF1820305 had provided partial support for the training and mentoring of 1 graduate (PhD) student (non-US citizen) and 1 undergraduate student (US citizen) in the academic year 2019 - 2020.

Partial support from the grant enabled the PhD candidate, Mr. Seyyed A. Davari to complete his PhD dissertation along with the publication of a high-impact journal article in Appl. Surf. Sci., 473, 156 [2019] toward the end of his PhD curriculum.

Support from the current grant also enabled the undergraduate student Mr. Elijah Davis - who had started his undergraduate engineering studies at a local community college in Knoxville, TN as part of an affordable college outreach program – to gain significant research experiences and knowledge in experimental synthesis and characterization of energetic nanomaterials. Such early-career STEM experiences provided the foundation for considerable professional and intellectual development in his early research career. Motivated by this research experience, Mr. Davis has now continued to pursue a PhD in the Chemical Engineering program at University of Tennessee, Knoxville since Fall 2020. His current research on LASiS-driven synthesis of advanced and novel ENMs is currently funded by AFOSR- and has led to high-impact results that have the potential to revolutionize the field. His research is being reviewed by OUSD’s ARAP-EEE program and has led to a manuscript under review with the Journal of DoD Research & Engineering (JDRE) as a limited distribution material. He has also had hands-on research experiences working very closely in collaboration with scientists and researchers from US Army Research Lab [ARL, Aberdeen], Argonne National Lab [ANL] and Oak Ridge National Lab [ORNL]. In sum, the current grant ARO grant bore an immediate impact in supporting and mentoring the career development goals for Elijah toward his PhD candidacy in the academic year of 2020, thereby preparing him to be a successful future scientific member contributing to US DoD’s national security missions.

RPPR Final Report
as of 12-Jul-2022

Results Dissemination: Results were disseminated during the period of performance of the current STIR grant via: 1 publication and 6 conference/symposium presentations (including 3 invited talks). The details are provided below:

Journal Publications:
S. A. Davari, J. L. Gottfried, C. Liu, E. L. Ribeiro, G. Duscher, D. Mukherjee, (2019) “Graphitic coated Al nanoparticles manufactured as superior energetic materials via laser ablation synthesis in organic solvents.” Applied Surface Science (Special Issue), 473, 156.
https://doi.org/10.1016/j.apsusc.2018.11.238.

Conference/Symposium Presentations:

A. Invited Talks:
1. Dibyendu Mukherjee*, “New frontiers for nano/biomaterials in energy, energetic and environmental studies,” Materials Sci. & Engg. Fall 2020 Colloquium, University of California, Riverside, Nov. 4, 2020.
2. Elijah Davis, Dibyendu Mukherjee*, “Designing Composite and Metastable Energetic Nanomaterials with Tunable Interfacial Activities via Laser Ablation Synthesis in Solution,” Computational Chemistry/ Modeling Meeting, US Army Engineer Research & Development Center (ERDC), Sept. 24, 2019, Vicksburg MS.
3. Dibyendu Mukherjee*, "Structurally designed metal/ceramic nanoparticles with tailored interfacial activities manufactured as superior energetic materials via laser ablation synthesis in solution," Eglin Air Force Base, Air Force Research Laboratory (AFRL), Dec. 4, 2018, Eglin FL.

B. Conferences:
1. Dibyendu Mukherjee*, Seyyed A. Davari, Jennifer L. Gottfried, Gerd Duscher, “Colloidal Synthesis of Al/C-Based Composite Energetic Nanoparticles with Tunable Interfacial Activities via Laser Ablation Synthesis in Solution,” 2020 Virtual MRS Spring/Fall Meeting (Online), Nov. 27-Dec. 4, 2020.
2. Dibyendu Mukherjee, “Designing Composite Energetic Nanomaterials with Tunable Interfacial Activities Via Laser Ablation Synthesis in Solution,” AIChE Annual Meeting, Nov.10-15, 2019, Orlando, FL.
3. Dibyendu Mukherjee, “Synthesis of composite energetic nanomaterials with tunable interfacial activities via laser ablation synthesis in solution,” U.S. Army Research Office (ARO): Molecular Structure & Dynamics Program Review, June 25 2019, Durham, NC.

Honors and Awards: Nothing to Report

Protocol Activity Status:

Technology Transfer: Nothing to Report

PARTICIPANTS:

Participant Type: Graduate Student (research assistant)
Participant: Seyyed A. Davari
Person Months Worked: 9.00 **Funding Support:**
Project Contribution:
National Academy Member: N

Participant Type: Undergraduate Student
Participant: Elijah Davis
Person Months Worked: 6.00 **Funding Support:**
Project Contribution:
National Academy Member: N

RPPR Final Report
as of 12-Jul-2022

ARTICLES:

Publication Type: Journal Article Peer Reviewed: Y **Publication Status:** 1-Published
Journal: Applied Surface Science
Publication Identifier Type: ISSN Publication Identifier: 0169-4332
Volume: 473 Issue: 1 First Page #: 156-163
Date Submitted: 7/6/22 12:00AM Date Published: 12/2/18 1:00AM
Publication Location:
Article Title: Graphitic coated Al nanoparticles manufactured as superior energetic materials via laser ablation synthesis in organic solvents.
Authors: S. A. Davari, J. L. Gottfried, C. Liu, E. L. Ribeiro, G. Duscher, D. Mukherjee
Keywords: Laser ablation synthesis in solution (LASiS); Organic solvents; Graphitic shell; Aluminum nanoparticles; Energetic nanocomposites.
Abstract: We report results on the synthesis of graphitic shell coated Al NPs (<20 nm) via laser ablation synthesis in solution (LASiS) to preserve high surface areas and interfacial properties of Al NPs. Herein, we use a high-energy laser to ablate Al pellets confined in either acetone or toluene to coat active Al NP core with graphitic shells generated from thermal pyrolysis of the organic solvents. Energetic activities of the C/Al NPs were tested via laser-induced air shock from energetic materials (LASEM) technique. We demonstrated that synthesis parameters such as organic solvents, laser flux and ablation times can be tuned to tailor NP sizes/aggregation with the aid of the C shell formations and, in turn, their energetic behavior. This study revealsynthesis-structure-property relations in LASiS-based synthesis of energetic nanoccapsules within graphitic shells that are safe to handle and can undergo kinetically controlled spontaneous energy release under desired conditions.
Distribution Statement: 5-Distribution authorized to DoD Components only
Acknowledged Federal Support: **Y**

CONFERENCE PAPERS:

Publication Type: Conference Paper or Presentation **Publication Status:** 0-Other
Conference Name: 2020 Virtual MRS Spring/Fall Meeting
Date Received: 06-Jul-2022 Conference Date: 27-Nov-2020 Date Published: 04-Dec-2020
Conference Location: Online (Virtual)
Paper Title: Colloidal Synthesis of Al/C-Based Composite Energetic Nanoparticles with Tunable Interfacial Activities via Laser Ablation Synthesis in Solution
Authors: Dibyendu Mukherjee, Seyyed A. Davari, Jennifer L. Gottfried, Gerd Duscher
Acknowledged Federal Support: **Y**

Publication Type: Conference Paper or Presentation **Publication Status:** 0-Other
Conference Name: 2019 AIChE Annual Meeting
Date Received: 06-Jul-2022 Conference Date: 10-Nov-2019 Date Published: 15-Nov-2019
Conference Location: Orlando, FL USA
Paper Title: Designing Composite Energetic Nanomaterials with Tunable Interfacial Activities Via Laser Ablation Synthesis in Solution
Authors: Dibyendu Mukherjee
Acknowledged Federal Support: **Y**

RPPR Final Report
as of 12-Jul-2022

Partners

,

I certify that the information in the report is complete and accurate:
Signature: Dibyendu Mukherjee
Signature Date: 7/6/22 5:09PM

BIBILOGRAPHY:

(1) B. A. Mason, L. J. Groven, S. F. Son, and R. A. Yetter; *"Combustion Performance of Several Nanosilicon-Based Nanoenergetics,"* Journal of Propulsion and Power, **2013**, *29*, 1435-1444.

(2) N. W. Piekiel, W. A. Churaman, C. J. Morris, and L. J. Currano; *"Combustion and Material Characterization of Porous Silicon Nanoenergetics,"* 26th Ieee International Conference on Micro Electro Mechanical Systems (Mems 2013), **2013**, 449-452.

(3) R. Thiruvengadathan, G. M. Belarde, A. Bezmelnitsyn, M. Shub, W. Balas-Hummers, K. Gangopadhyay, and S. Gangopadhyay; *"Combustion Characteristics of Silicon-Based Nanoenergetic Formulations with Reduced Electrostatic Discharge Sensitivity,"* Propellants Explosives Pyrotechnics, **2012**, *37*, 359-372.

(4) L. Zhou, N. Piekiel, S. Chowdhury, and M. R. Zachariah; *"Time-Resolved Mass Spectrometry of the Exothermic Reaction between Nanoaluminum and Metal Oxides: The Role of Oxygen Release,"* Journal of Physical Chemistry C, **2010**, *114*, 14269-14275.

(5) K. Sullivan, G. Young, and M. R. Zachariah; *"Enhanced reactivity of nano-B/Al/CuO MIC's,"* Combustion and Flame, **2009**, *156*, 302-309.

(6) A. Prakash, A. V. McCormick, and M. R. Zachariah; *"Synthesis and reactivity of a super-reactive metastable intermolecular composite formulation of Al/KMnO4,"* Advanced Materials, **2005**, *17*, 900-+.

(7) A. Prakash, A. V. McCormick, and M. R. Zachariah; *"Tuning the reactivity of energetic nanoparticles by creation of a core-shell nanostructure,"* Nano Letters, **2005**, *5*, 1357-1360.

(8) A. Prakash, A. V. McCormick, and M. R. Zachariah; *"Aero-sol-gel synthesis of nanoporous iron-oxide particles: A potential oxidizer for nanoenergetic materials,"* Chemistry of Materials, **2004**, *16*, 1466-1471.

(9) D. Mukherjee, A. Rai, and M. R. Zachariah; *"Quantitative laser-induced breakdown spectroscopy for aerosols via internal calibration: Application to the oxidative coating of aluminum nanoparticles,"* Journal of Aerosol Science, **2006**, *37*, 677-695.

(10) K. Park, D. Lee, A. Rai, D. Mukherjee, and M. R. Zachariah; *"Size-resolved kinetic measurements of aluminum nanoparticle oxidation with single particle mass spectrometry,"* Journal of Physical Chemistry B, **2005**, *109*, 7290-7299.

(11) D. Mukherjee, M. Wang, and B. Khomami; *"Impact of particle morphology on surface oxidation of nanoparticles: A kinetic Monte Carlo based study,"* Aiche Journal, **2012**, *58*, 3341-3353.

(12) D. Mukherjee, A. Prakash, and M. R. Zachariah; *"Implementation of a discrete nodal model to probe the effect of size-dependent surface tension on nanoparticle formation and growth,"* Journal of Aerosol Science, **2006**, *37*, 1388-1399.

(13) D. Mukherjee, C. G. Sonwane, and M. R. Zachariah; *"Kinetic Monte Carlo simulation of the effect of coalescence energy release on the size and shape evolution of nanoparticles grown as an aerosol,"* Journal of Chemical Physics, **2003**, *119*, 3391-3404.

(14) H. R. Leverentz, J. I. Siepmann, D. G. Truhlar, V. Loukonen, and H. Vehkamaki; *"Energetics of Atmospherically Implicated Clusters Made of Sulfuric Acid, Ammonia, and Dimethyl Amine,"* Journal of Physical Chemistry A, **2013**, *117*, 3819-3825.

(15) Donald F. Johnson, and William D. Mattson; *"Theoretical investigations of surface reconstruction on C nanodiamonds and cubic-BN nanoparticles,"* Diamond and Related Materials, **2015**, *58*, 155-160.

(16) D. Golberg, Y. Bando, T. Sato, N. Grobert, M. Reyes-Reyes, H. Terrones, and M. Terrones; *"Nanocages of layered BN: Super-high-pressure nanocells for formation of solid nitrogen,"* Journal of Chemical Physics, **2002**, *116*, 8523-8532.

(17) A. Rai, D. Lee, K. H. Park, and M. R. Zachariah; *"Importance of phase change of aluminum in oxidation of aluminum nanoparticles,"* Journal of Physical Chemistry B, **2004**, *108*, 14793-14795.

(18) Kihong Park, Ashish Rai, and MR Zachariah; *"Characterizing the coating and size-resolved oxidative stability of carbon-coated aluminum nanoparticles by single-particle mass-spectrometry,"* Journal of Nanoparticle Research, **2006**, *8*, 455-464.

(19) Dibyendu Mukherjee, and Sheng Hu; Compositions, Systems and Methods for Producing Nanoalloys, and/or Nanocomposites using tandem Laser Ablation Synthesis in Solution-Galvanic Replacement Reaction, **Patent No: 20170296997A1**, **USA**, **2016**.

(20) Sheng Hu, Mengkun Tian, Erick L. Ribeiro, Gerd Duscher, and Dibyendu Mukherjee; *"Tandem laser ablation synthesis in solution-galvanic replacement reaction (LASiS-GRR) for the production of PtCo nanoalloys as oxygen reduction electrocatalysts,"* Journal of Power Sources, **2016**, *306*, 413-423.

(21) Sheng Hu, Gabriel Goenaga, Chad Melton, Thomas A. Zawodzinski, and Dibyendu Mukherjee; *"PtCo/CoOx nanocomposites: Bifunctional electrocatalysts for oxygen reduction and evolution reactions synthesized via tandem laser ablation synthesis in solution-galvanic replacement reactions,"* Applied Catalysis B: Environmental, **2016**, *182*, 286-296.

(22) S. Hu, C. Melton, and D. Mukherjee; *"A facile route for the synthesis of nanostructured oxides and hydroxides of cobalt using laser ablation synthesis in solution (LASIS),"* Physical Chemistry Chemical Physics, **2014**, *16*, 24034-24044.

(23) S. Hu, E. L. Ribeiro, S. A. Davari, M. K. Tian, D. Mukherjee, and B. Khomami; *"Hybrid nanocomposites of nanostructured Co3O4 interfaced with reduced/nitrogen-doped graphene oxides for selective improvements in electrocatalytic and/or supercapacitive properties,"* Rsc Advances, **2017**, *7*, 33166-33176.

(24) S. Hu, K. M. Cheng, E. L. Ribeiro, K. Park, B. Khomami, and D. Mukherjee; *"A facile and surfactant-free route for nanomanufacturing of tailored ternary nanoalloys as superior oxygen reduction reaction electrocatalysts,"* Catalysis Science & Technology, **2017**, *7*, 2074-2086.
(25) J. L. Gottfried; *Laboratory-Scale Method for Estimating Explosive Performance from Laser-Induced Shock Waves.* Propellants, Explosives, Pyrotechnics, **2015**. **40**(5): p. 674-681.
(26) J. L. Gottfried, T.M. Klapötke, and T.G. Witkowski; *Estimated Detonation Velocities for TKX-50, MAD-X1, BDNAPM, BTNPM, TKX-55, and DAAF using the Laser–induced Air Shock from Energetic Materials Technique.* Propellants, Explosives, Pyrotechnics, **2017**. **42**(4): p. 353-359.
(27) J. L. Gottfried, and E.J. Bukowski; *Laser-shocked energetic materials with metal additives: evaluation of chemistry and detonation performance.* Applied optics, **2017**. **56**(3): p. B47-B57.

FIGURES:

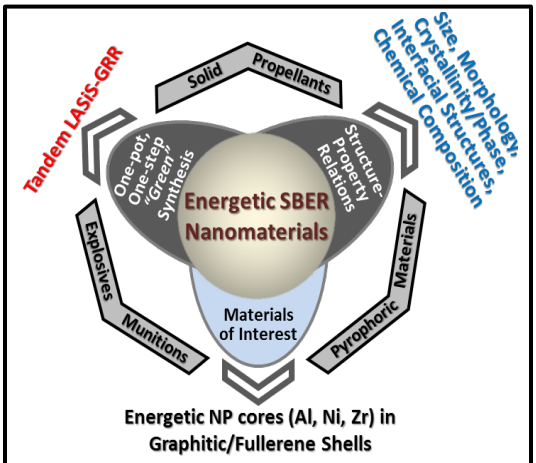

Fig. 1 Overview of Research Goals

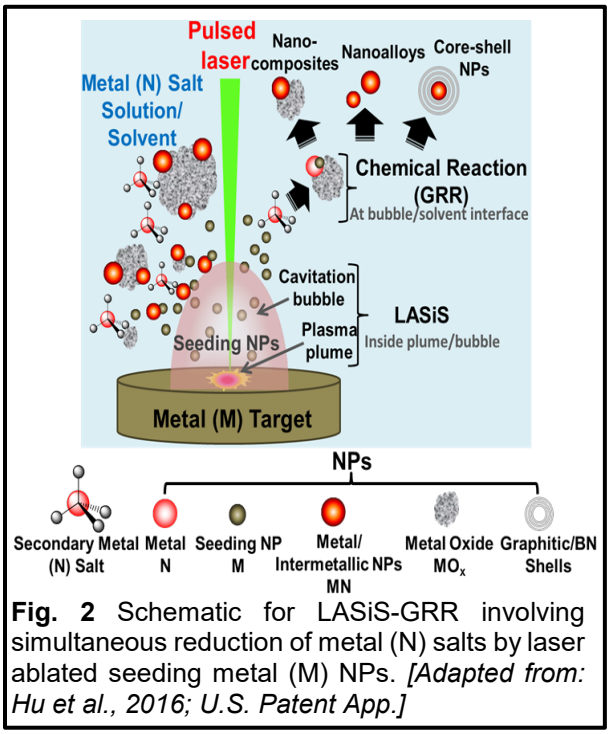

Fig. 2 Schematic for LASiS-GRR involving simultaneous reduction of metal (N) salts by laser ablated seeding metal (M) NPs. *[Adapted from: Hu et al., 2016; U.S. Patent App.]*

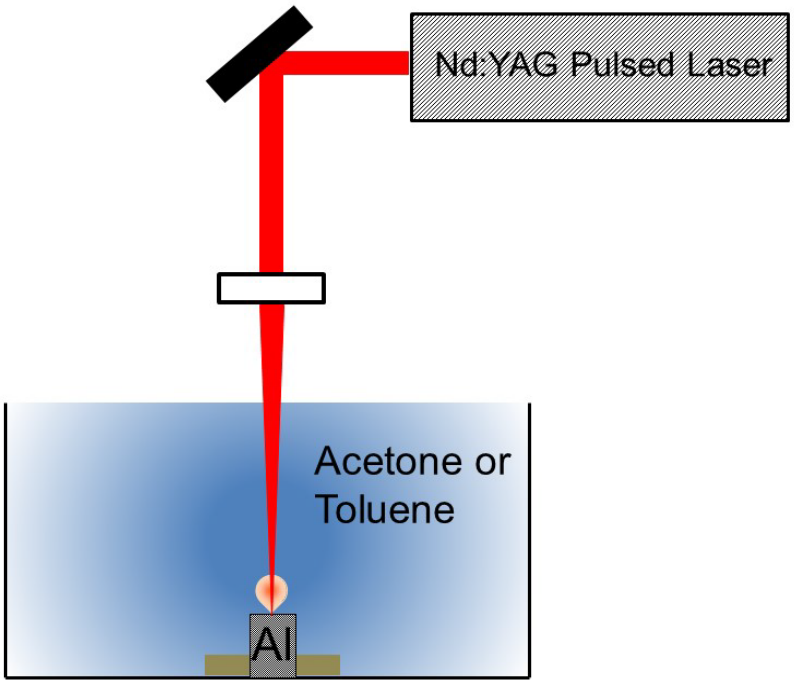

Fig 3. Schematic for the in-house developed LASiS set-up.

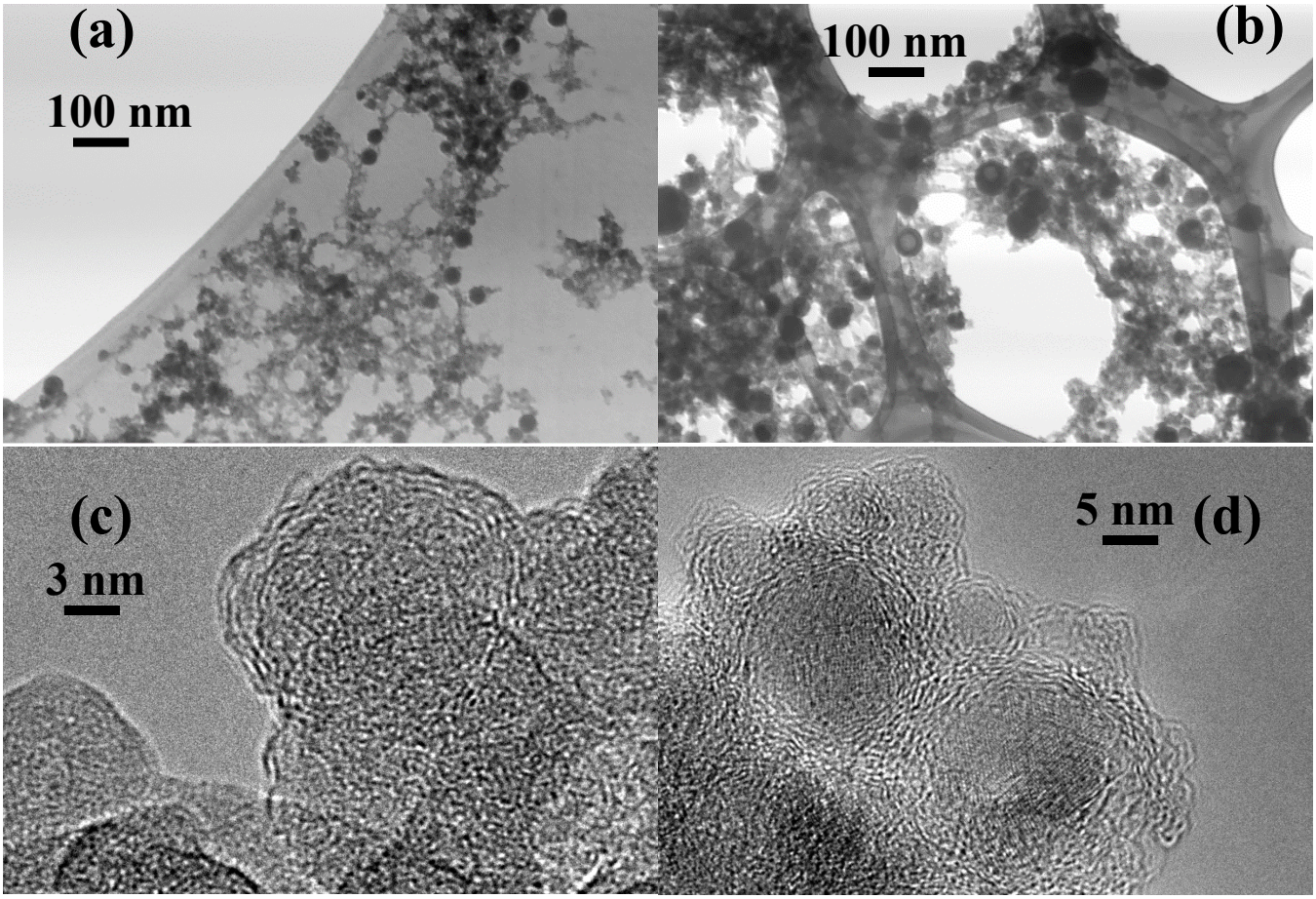

Fig. 4. Scanning transmission electron microscope (STEM) images of composite C/Al NP samples prepared via LASiS in **(a)** acetone and **(b)** toluene. High-resolution transmission electron microscope (HRTEM) images of composite C/Al NP samples prepared via LASiS in **(c)** acetone and **(d)** toluene.

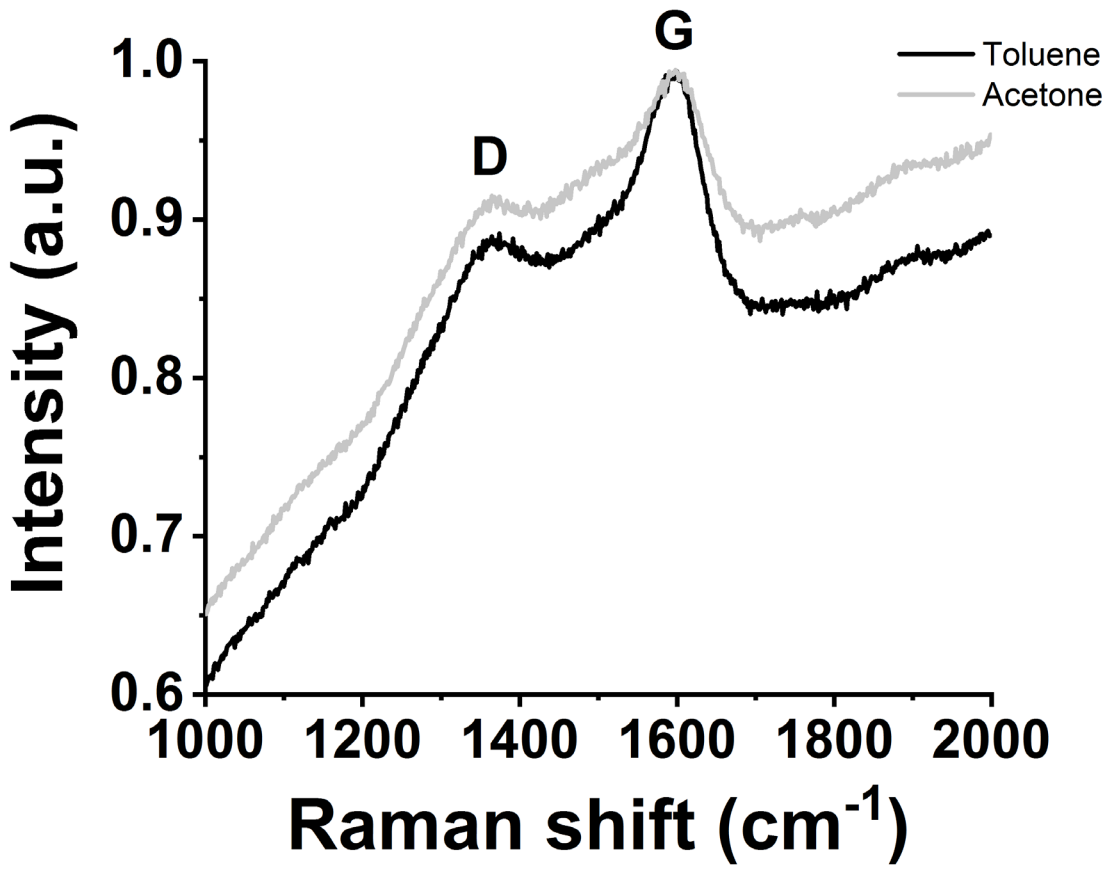

Fig. 5. Raman spectra for the samples prepared in acetone or toluene; labels indicate the well-known D and G bands for carbon.

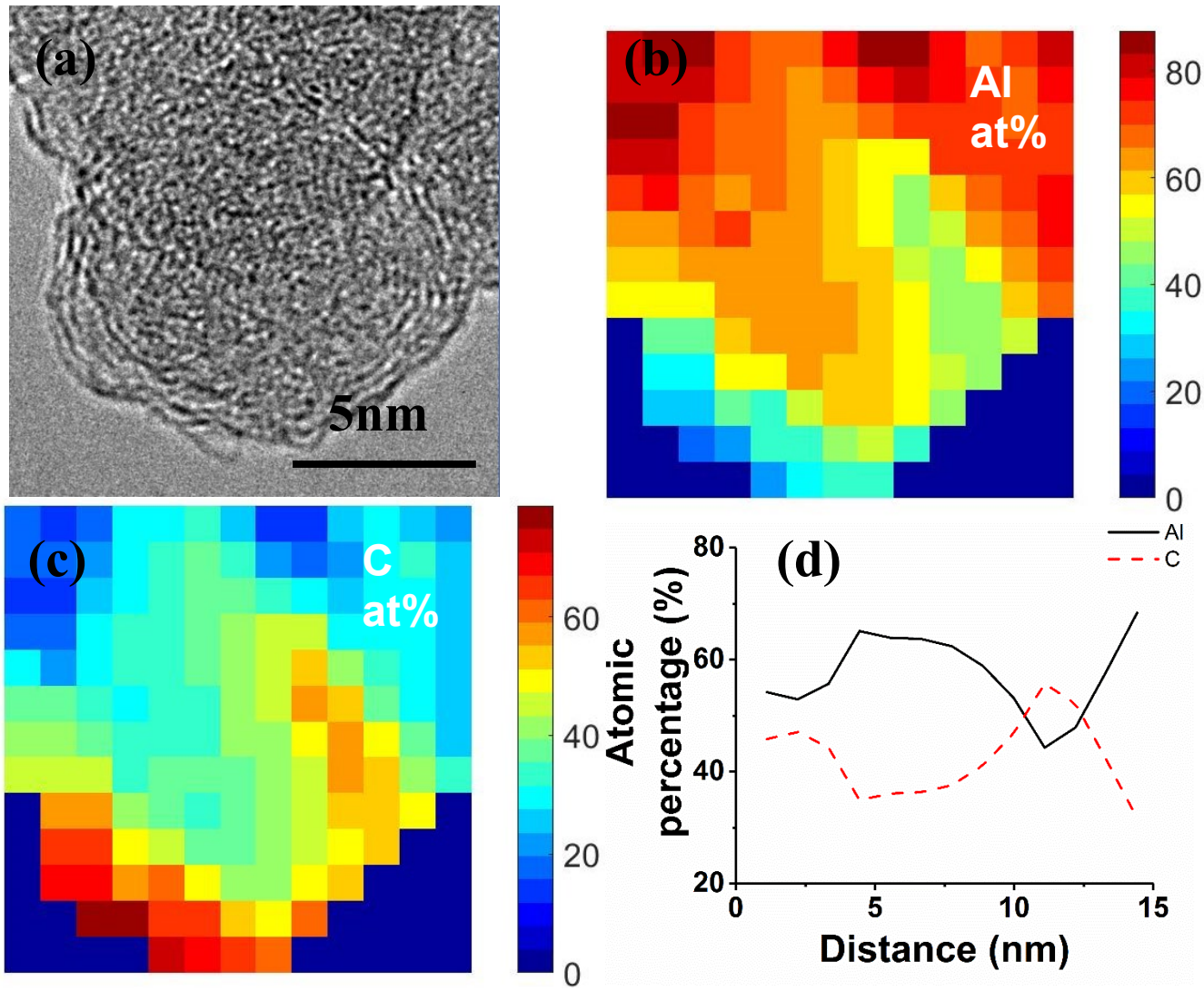

Fig. 6. (a) HRTEM image of the Al/C composite prepared in acetone indicating graphitic shell coatings on the Al NP core. EELS elemental mapping for the corresponding species **(b)** Al or **(c)** C. The atomic ratio (%) distributions for Al (solid black line) and C (dashed red line) across the line scan are shown in **(d)**.

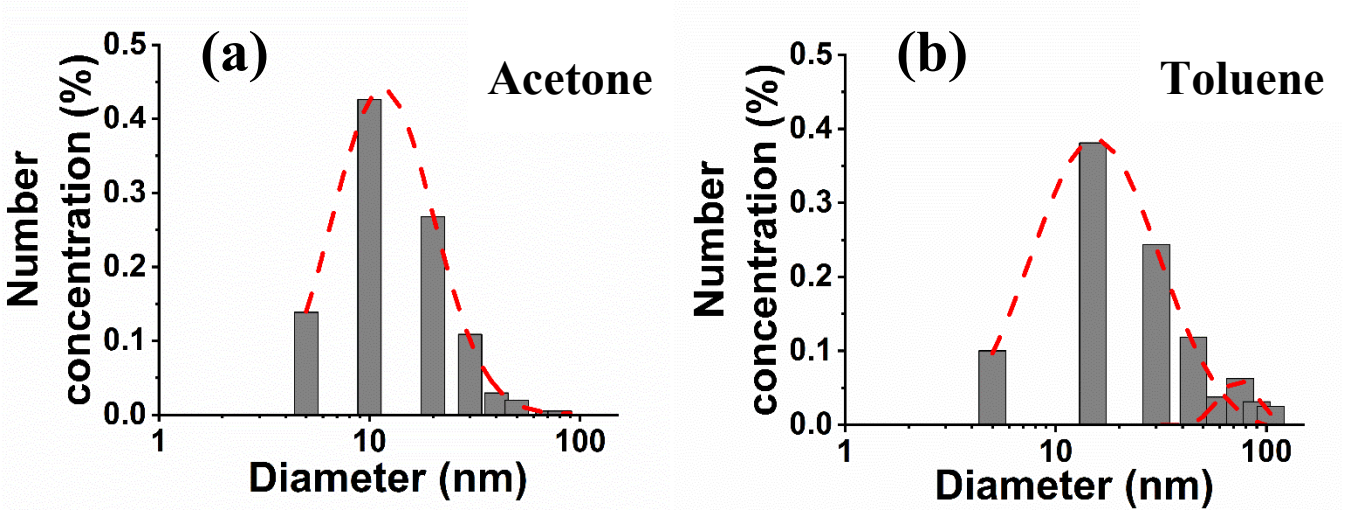

Fig. 7. Effect of organic solvents on the size distributions of the C/Al NPs prepared in **(a)** acetone and **(b)** toluene for ablation at a laser fluence of 2.6 J/cm^2 for 4 min.

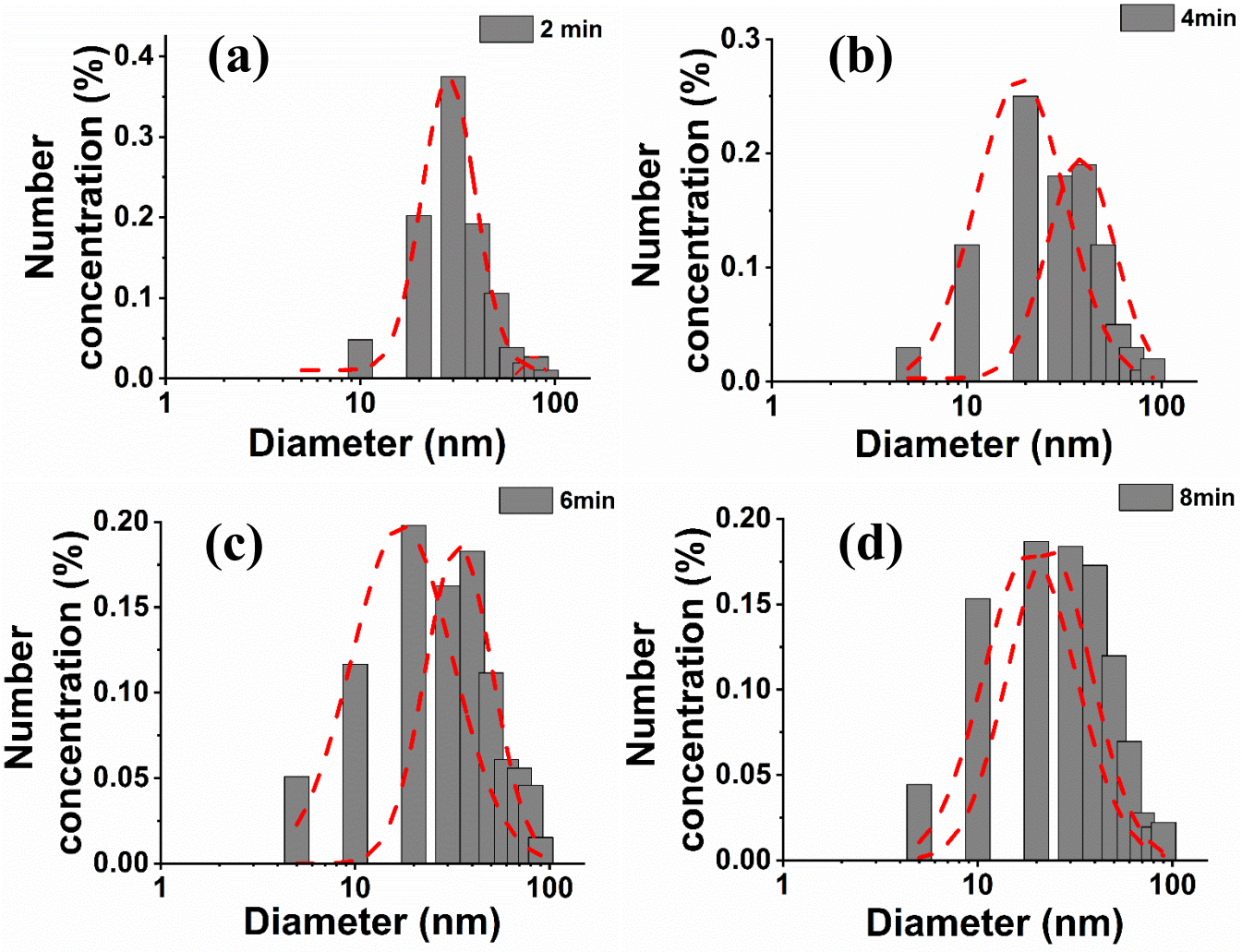

Fig. 8. Effect of laser ablation time on size distribution of the C/Al NPs prepared from LASiS in toluene at 2 J/cm laser fluence.

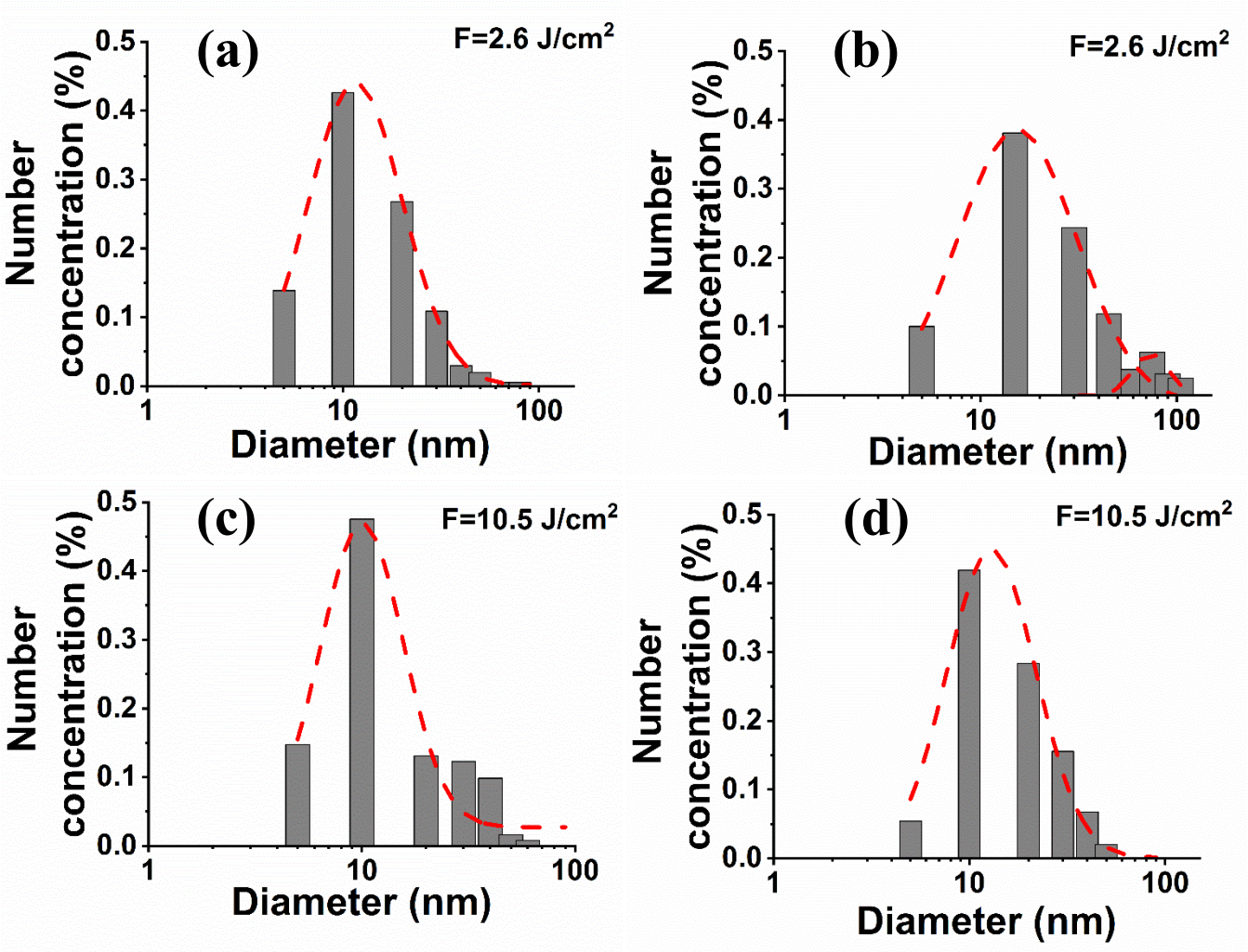

Fig. 9. Effect of laser fluence (F, J/cm^2) on the size distribution of C/Al NPs prepared via LASiS in **(a & c)** acetone and **(b & d)** in toluene.

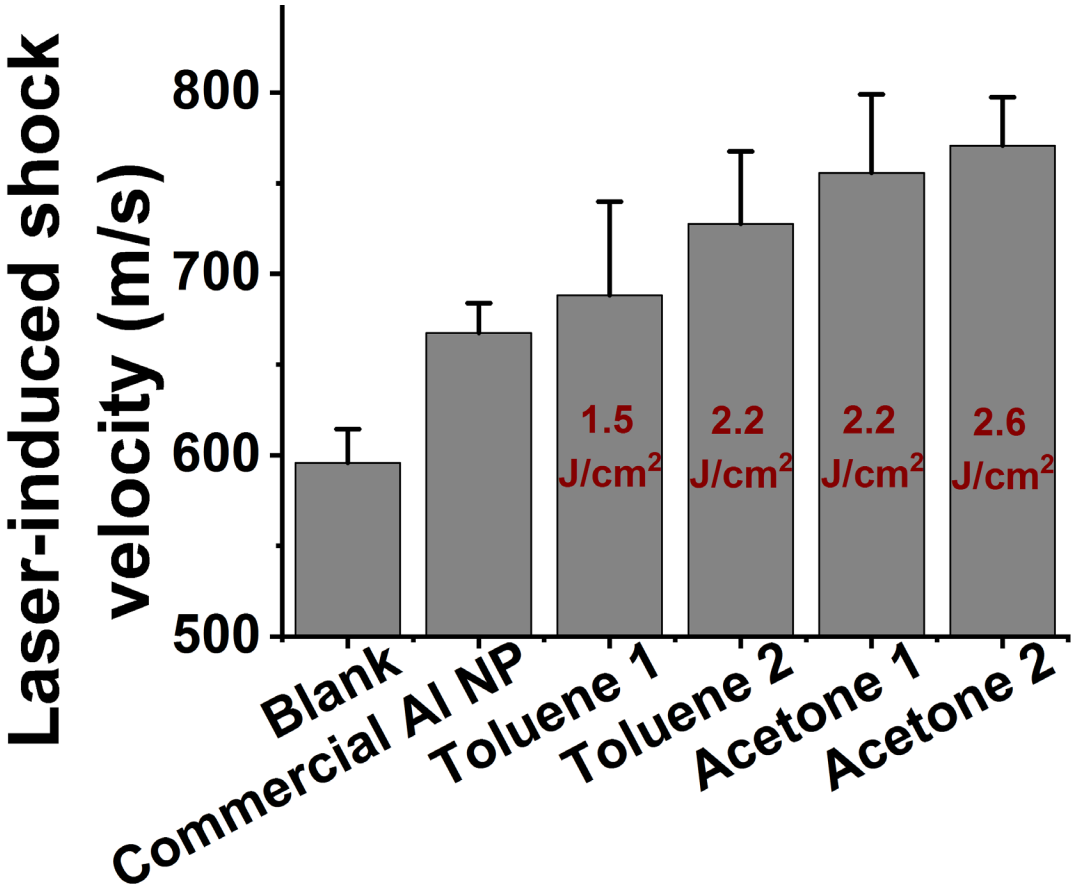

Fig. 10. Comparison of laser-induced shock velocities from LASEM measurements on samples prepared in acetone or toluene at various laser fluences, as compared to commercial nano-Al powders and the blank substrate.

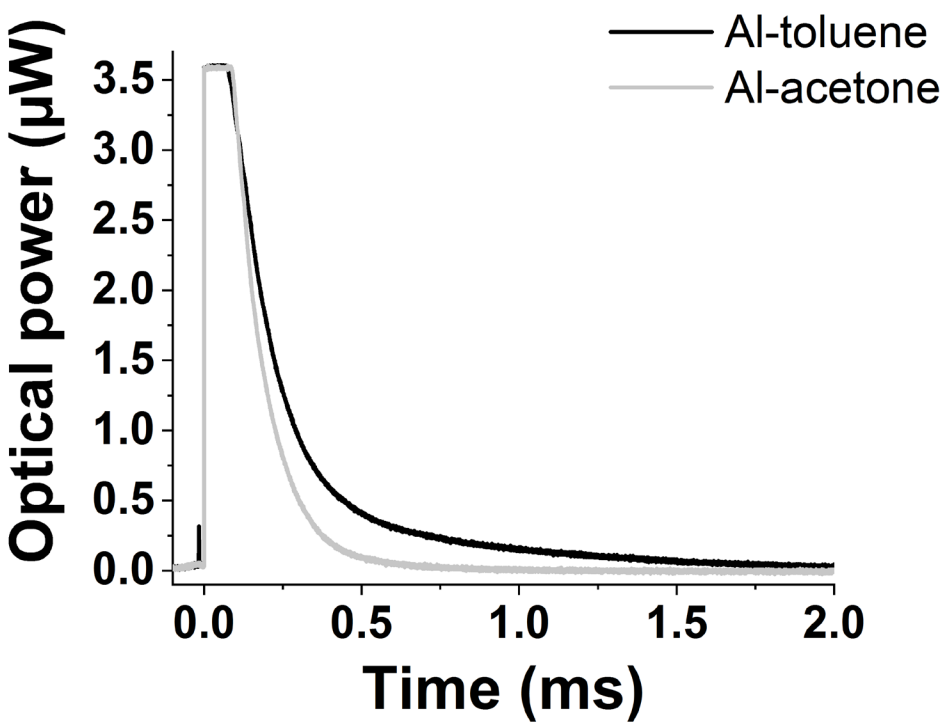

Fig. 11. Time-resolved emission from the reaction of laser-excited C/Al NPs prepared in toluene or acetone.

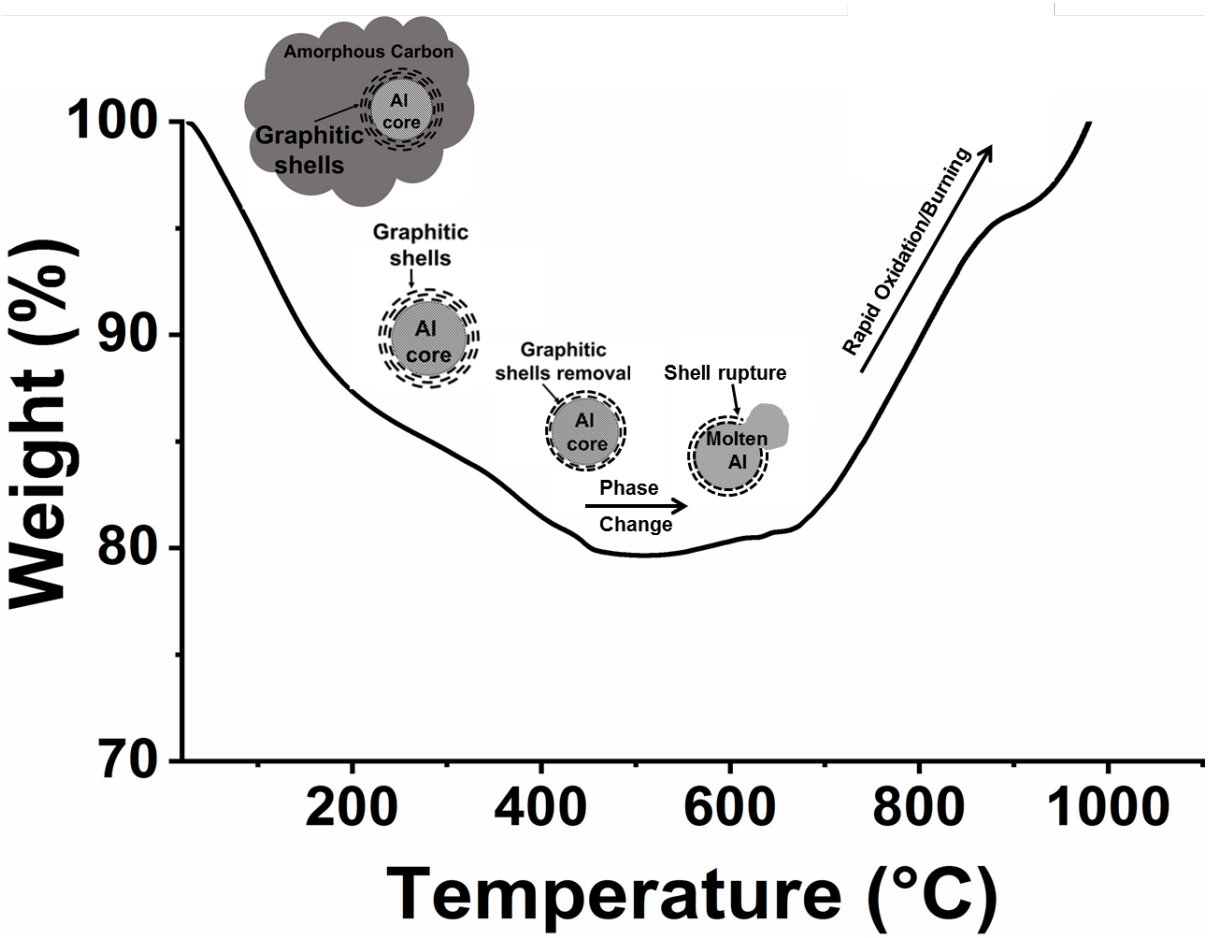

Fig. 12. TGA analysis for the sample with highest LASEM activity (acetone, 2.6 J/cm^2)

Penta Chart and Presentation Slides from **U.S. Army Research Office (ARO), Molecular Structure & Dynamics Program Review; 25 June 2019; Durham, NC**

Synthesis of composite energetic nanomaterials with tunable interfacial activities via laser ablation synthesis in solution (LASiS)

Graphitic shell coated composite Al/C NPs as energetic nanomaterials (ENMs)

STATUS QUO

➢ **1st Gen Energetic Al NPs: Problems**

- Preserving interfacial activities
- Unwanted oxide shell formation
- Diffusion-limited oxidation
- Excess aggregation

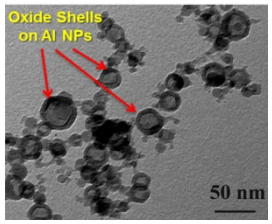

➢ **Existing Challenge:**

Design and facile synthesis of composite ENMs passivated in graphitic shells with kinetically controlled activation

NEW INSIGHTS

- Tunable passivation & activation.
- Stabilization of NPs by C matrix.
- Structure-property relations in composite Al/C ENMs tuned via suitable choice of solvents (Acetone, Toluene), laser fluence and ablations times in LASiS.
- Composition (Al/C/O %wt) & crystalline structures of metastable Al/Al_4C_3 NPs encapsulated in C matrix dictate exothermic/explosive behavior.

MAIN ACHIEVEMENTS:

- Developed chemically clean, facile LASiS technique to synthesize graphitic shell coated composite Al/C NPs in C matrix as superior ENMs.
- Superior performance metrics as compared to commercial energetic Al NPs. Max. laser-induced shock wave velocity **~796.57±9.33 m/s** exceeded desired energetic metrics (>650 m/s).
- ENM size, shape, composition and crystalline structures controlled via solvent and laser parameters.
- Combustion kinetics & thermodynamics tuned via heteronanostructuring of composite Al/C ENMs.

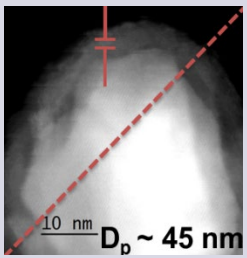

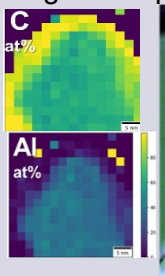

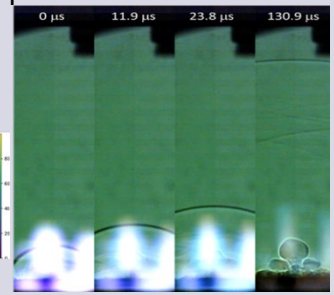

HOW IT WORKS:

- Activation @ 150-200°C burns off C shell/matrix
- Enhances the combustion
- Gaseous by-products (CO_2, CO etc.)
- Graphitic shell hinders coarsening

ASSUMPTIONS AND LIMITATIONS:

- Tailoring accurately the NP compositions (Al/Al_4C_3%wt), interfacial structures and shell thickness.
- Tuning metastable states with Al,C,O ratios to kinetically trap the ENMs.

QUANTITATIVE IMPACT

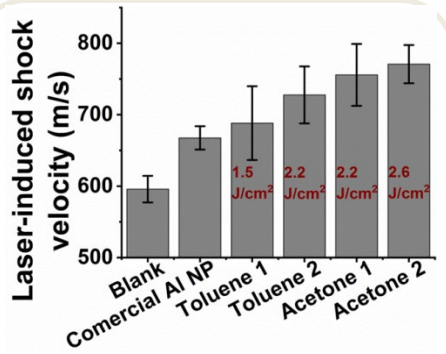

- Max. shock wave velocities from combustion **~796.57±9.33 m/s.**
- Net heat release and kinetics of the ENMs can be tuned via metastable states, compositions and crystalline structures.

END-OF-PHASE GOAL

➢ Tailoring accurate composition of Al/C/O ratios for the ENMs.

➢ Tuning detonation thermodynamics (*amount of heat release*) and kinetics (*rate of heat release*) by tailoring metastable states and crystalline structures for the composite Al/C ENMs.

➢ Exceed **combustion shock wave velocities > 1000 m/s**

KEY PUBLICATIONS: 1) S. A. Davari, et al. *Graphitic coated Al nanoparticles manufactured as superior energetic materials via laser ablation synthesis in organic solvents,* **Appl. Surf. Sci. (2019)**; **2)** S. Hu, et al., *Hybrid nanocomposites of nanostructured Co_3O_4 interfaced with reduced/nitrogen-doped graphene oxides for selective improvements in electrocalatytic and/or supercapacitive properties,* **RSC Adv. (2017).**

Synthesis of composite energetic nanomaterials with tunable interfacial activities via laser ablation synthesis in solution

Dibyendu Mukherjee

Nano-**B**io**M**aterials **L**aboratory for **E**nergy, **E**nergetics & **E**nvironment **(nbml-E^3)**

Department of Mechanical, Aerospace & Biomedical Engineering

University of Tennessee, Knoxville

U.S. Army Research Office (ARO)

Molecular Structure & Dynamics Program Review

25 June 2019; Durham, NC

Interfacial Energetics of Nanomaterials

Unique Nano-scale Characteristics :

- ❑ Small size scales → Large surface-to-volume ratio *(40% of atoms on surface for 1000 atom particle)*
- ❑ Small diffusion length scales → Shorter reaction time scale
- ❑ Excess energy of surface atoms → Reduced activation energy
- ❑ Metal/metal oxide NPs: Neither atomic species represented by well-defined molecular orbitals, nor standard bulk materials represented by electronic band structures → Size-dependent broadened energy states.

Unique Interfacial Properties:

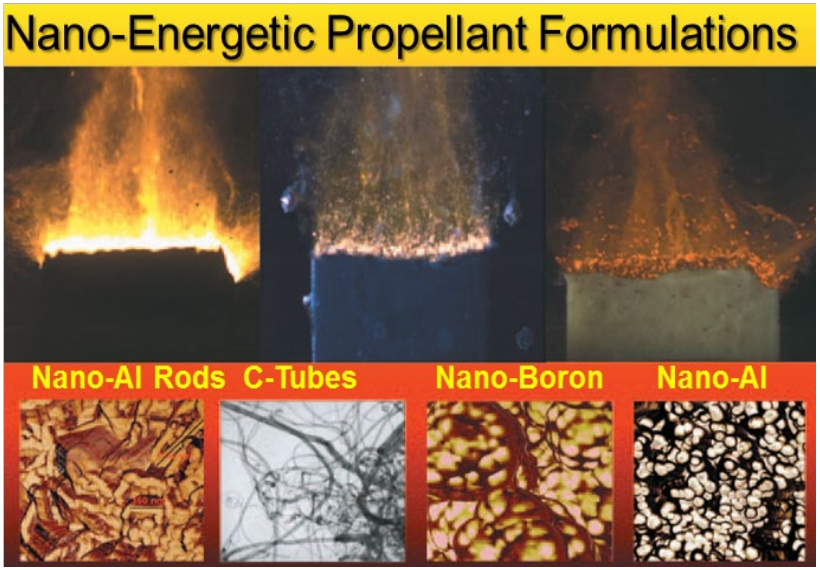

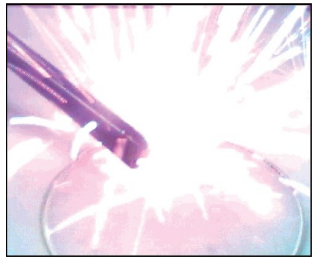

Prakash et al., **Chem. Mater. (2004)**

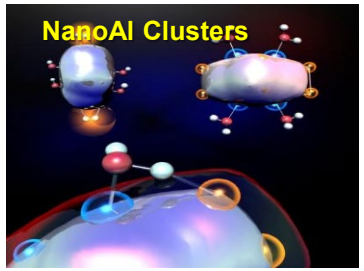

Roach et al., **Science (2009)**

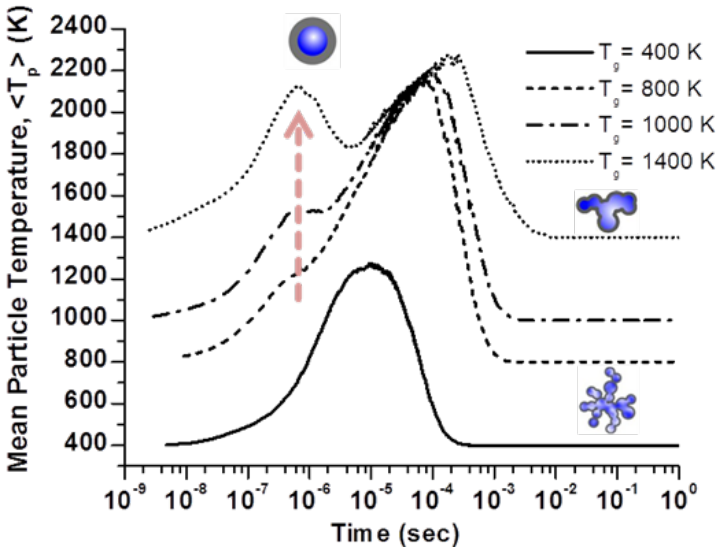

Mukherjee et al., **J. Chem Phys (2003); AIChE J. (2012)**

Tailor morphology (size/shape) during synthesis **(Physical Characterization)** ⟺ Tune surface gas-solid reactivity/adsorption (kinetics) **(Chemical Characterization)**

Understand interfacial physics and chemistry in nanomaterials

Facile, "Green" Synthesis of Energetic Nanomaterials (ENMs)

Knowledge Gap

Tandem Laser Ablation Synthesis in Solution-Galvanic Replacement Reactions (LASiS-GRR)

Current Solution-phase Synthesis Routes

- Use of unwanted chem…

Tandem LASiS-GRR

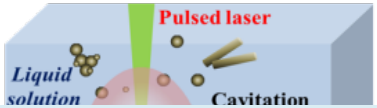

Future "Green" and Facile Synthesis Routes

Advanced composite NPs with tailored interfacial structures as ENMs

- Devoid of external chemicals , surfactants/ligands
- …e-pot, one-step synthesis
- …t-of-equilibrium (Metastable) structures
- …sired structure-composition-property relations
- …tarded aggregation due to charge stabilization
- …ergy efficient ~ 0.5 MJ/kg of NP production

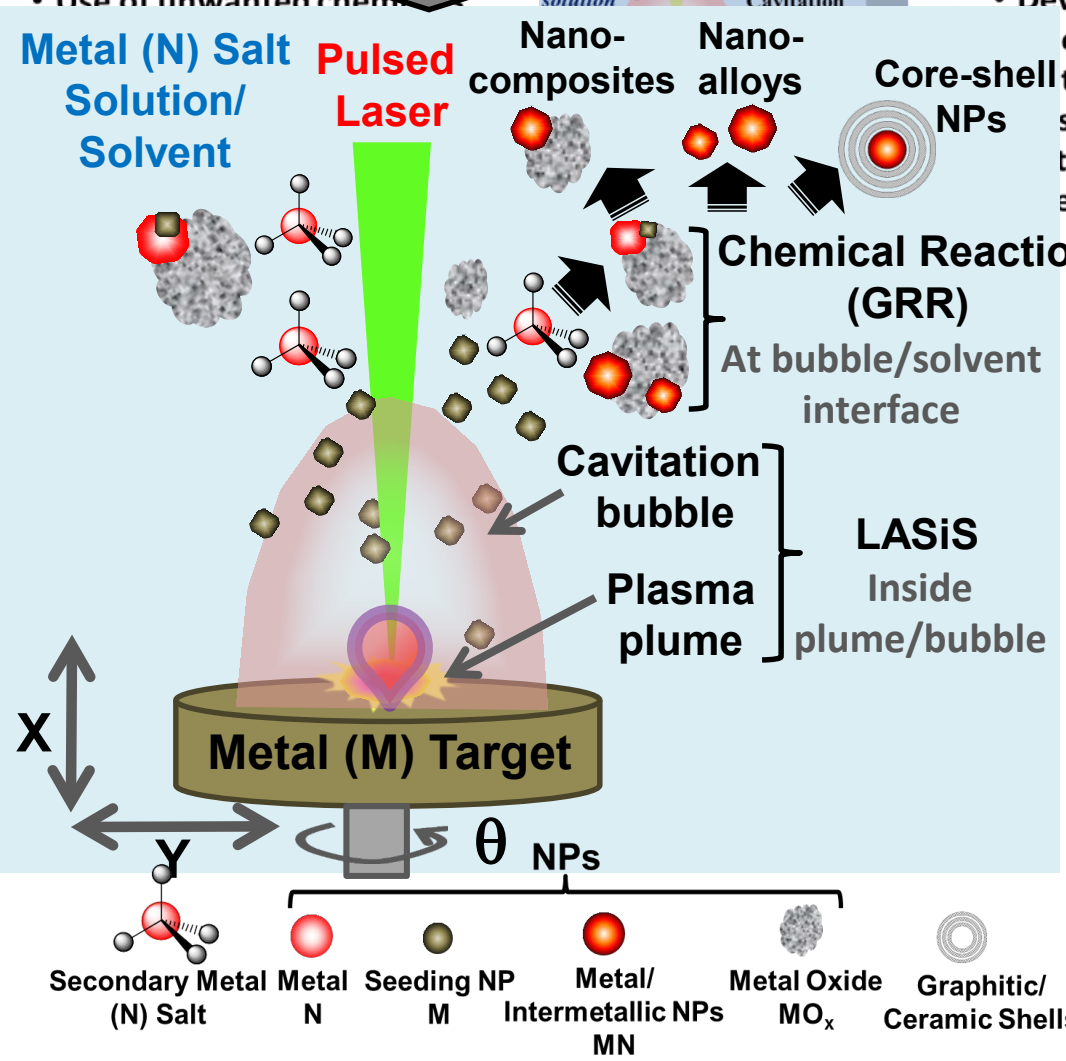

Technical Merit

- Disruptive *"top-down"* **LASiS** + *"bottom-up"* **GRR**
- High-energy laser-induced chemical physics *(T ~ 4000-5000 K; P ~ 10-15 GPa)*
- Process controls via laser and solvent chemistry
- Scalability via rate-controlled reaction kinetics

S. Hu, D. Mukherjee, **U.S. Patent Appl. 15/132,916, Issued, Pat No: 10326146 (2019)**

Versatility of LASiS-GRR

Functional nanomaterials synthesized so far:

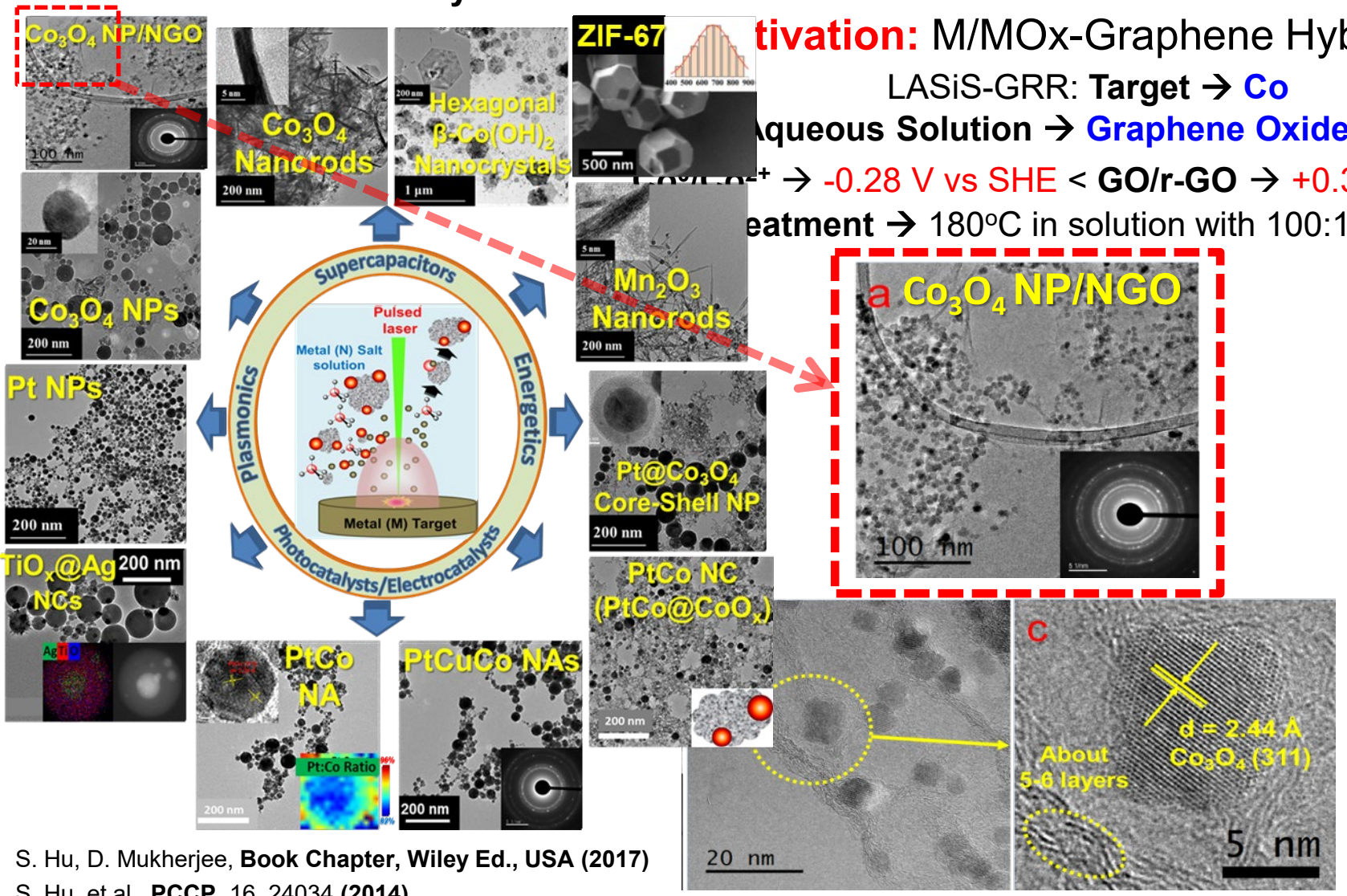

tivation: M/MOx-Graphene Hybrid NCs

LASiS-GRR: **Target** → **Co**

queous Solution → **Graphene Oxide (GO)**

$^{2+}$ → -0.28 V vs SHE < **GO/r-GO** → +0.35 V vs SHE

eatment → 180°C in solution with 100:1(urea : GO)

S. Hu, D. Mukherjee, **Book Chapter, Wiley Ed., USA (2017)**

S. Hu, et al., **PCCP,** 16, 24034 **(2014)**

S. Hu et al., **Appl. Catal. B,** 182, 286 **(2016)**

S. Hu et al., **J. Power Sources,** 306, 413 **(2016)**

S. Hu, et al., **Catal. Sci. Tech.,** 7, 2074 **(2017)**

E. L. Ribeiro, et al., **Mat. Chem. Frontiers (2019)**

Bifunctional Properties:

- ORR Fuel Cell Catalysis
- Supercapacitive properties

S. Hu et al., **RSC Adv.**, 7, 33166 **(2017)**

Energetic Metal Nanoparticles: Earlier work with Al NPs

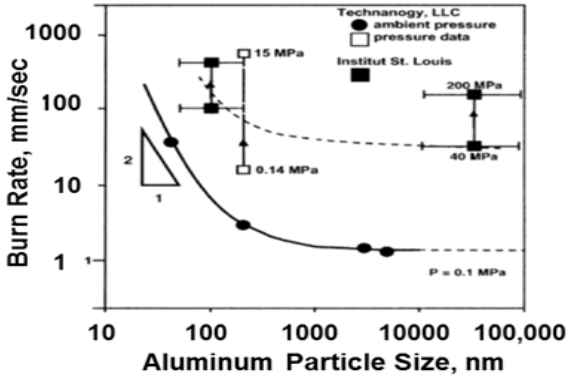

Armstrong et al., **Nano Lett, 2003**

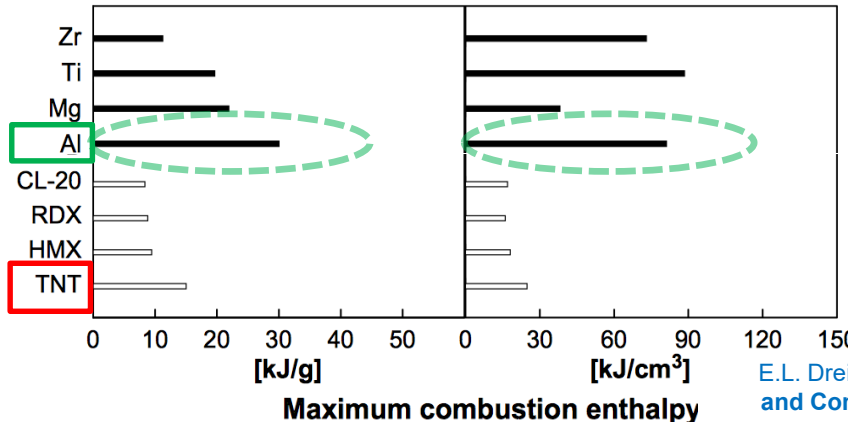

E.L. Dreizin, **Progress in Energy and Combustion Science, 2009**

Experimental:

- Gas-phase laser ablation synthesis of ENMs
- Oxidation kinetics analysis using laser-induced breakdown spectroscopy and mass spectrometry

Computational:

Comprehensive Kinetic Monte-Carlo (KMC) model:

- Nucleation
- Coagulation + Non-Isothermal Coalescence
- Surface oxidation

S. A. Davari, D. Mukherjee, ***Book Chapter in Energetic Materials***, Ed. M. Shukla, **Springer (2017)**

K. Park, D. Lee, A. Rai, D. Mukherjee, M.R. Zachariah, **J. Phys. Chem. B (2004)**

D. Mukherjee, C. G. Sonwane, M. R. Zachariah, **J. Chem. Phys. (2003)**

D. Mukherjee, A. Prakash, M. R. Zachariah, **J. Aerosol Sci. (2006)**

D. Mukherjee, A. Rai, M. R. Zachariah, **J. Aerosol Sci. (2006)**

D. Mukherjee, M. Wang, B. Khomami **AiChE J. (2012)**

S. A. Davari, D. Mukherjee, **AiChE J. (2018)**

➢ Problems with 1st Gen Energetic Al NPs:

- Preserving interfacial activities
- Unwanted oxide shell formation
- Diffusion-limited oxidation
- Surface area loss from excess aggregation

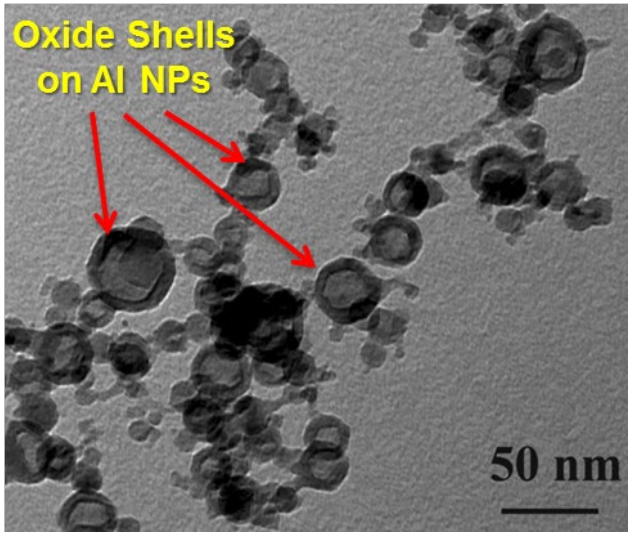

A. Rai, K. Park, L. Zhou, M.R. Zachariah
Combust. Th. Model., (2006)

Graphitic shell coated Al NPs: Next Gen ENMs

Basic Idea

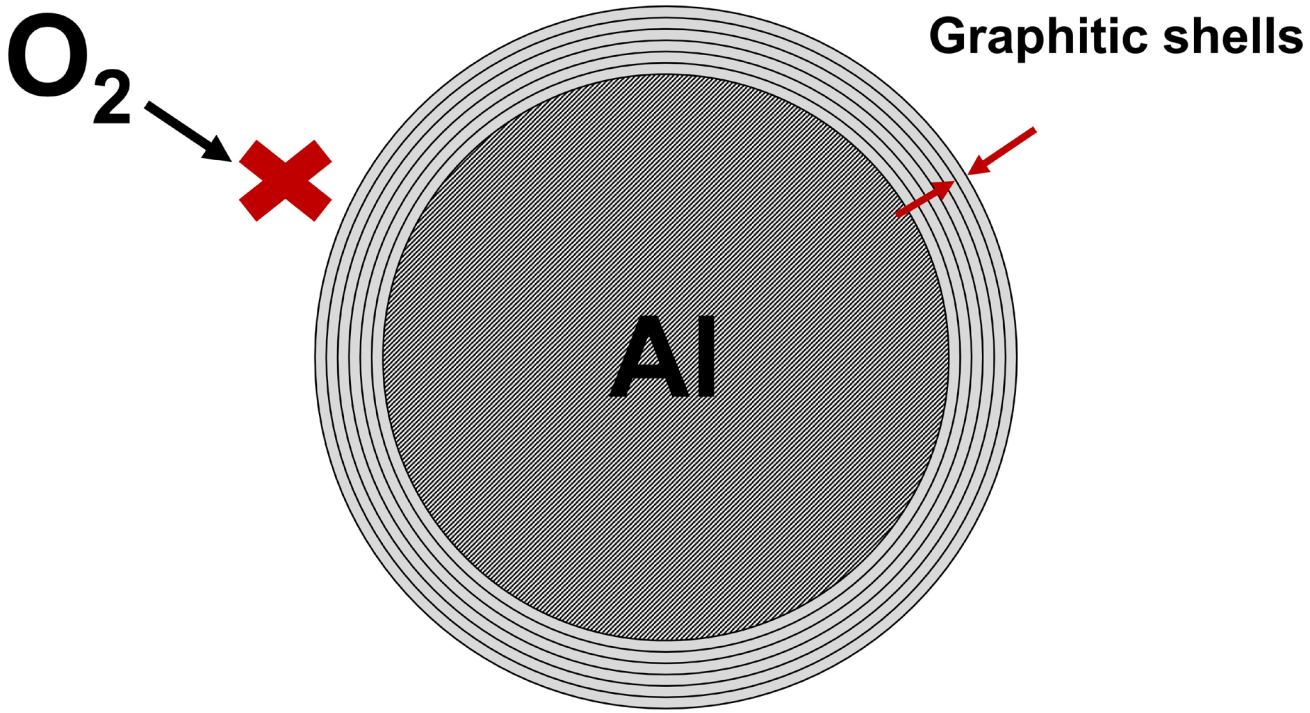

- Burns off C shell
- Enhances the combustion
- Gaseous by-products (CO_2, CO etc)
- Graphitic shell hinders coarsening

Graphitic shell coated Al NPs: Next Gen ENMs

LASiS-GRR: **Target → Al + Solvent → Toluene, Acetone** → *Pyrolysis of solvents*

- **Morphology and Structure:**

High Angle Annular Dark Field –STEM Imaging

Acetone

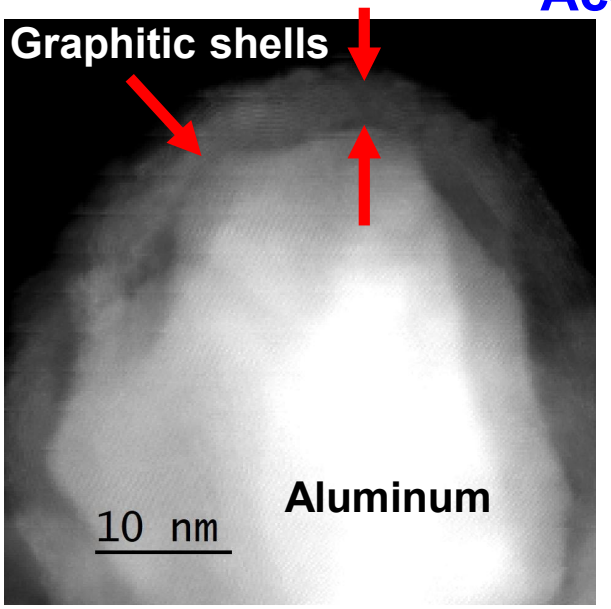

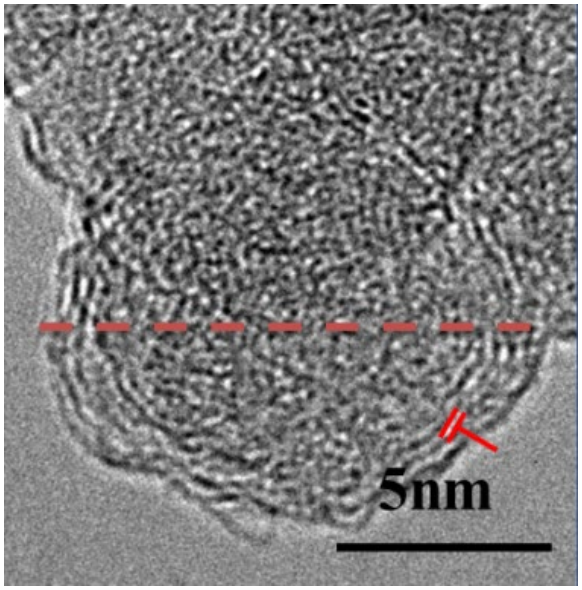

Raman Spectroscopy

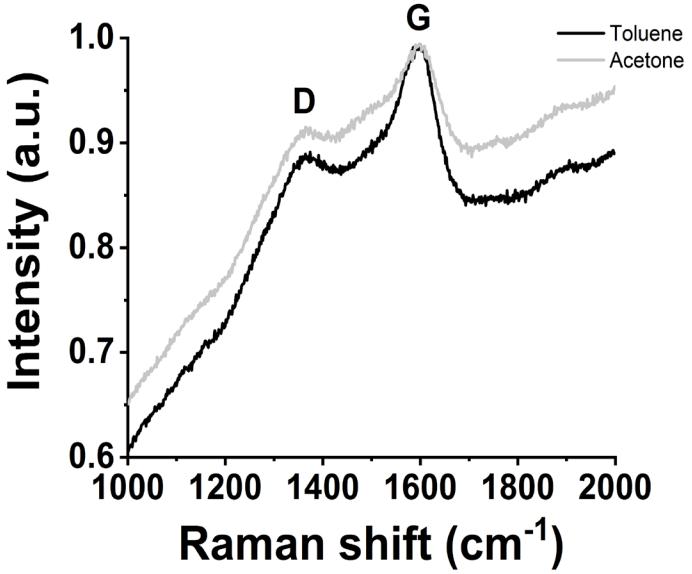

Toluene

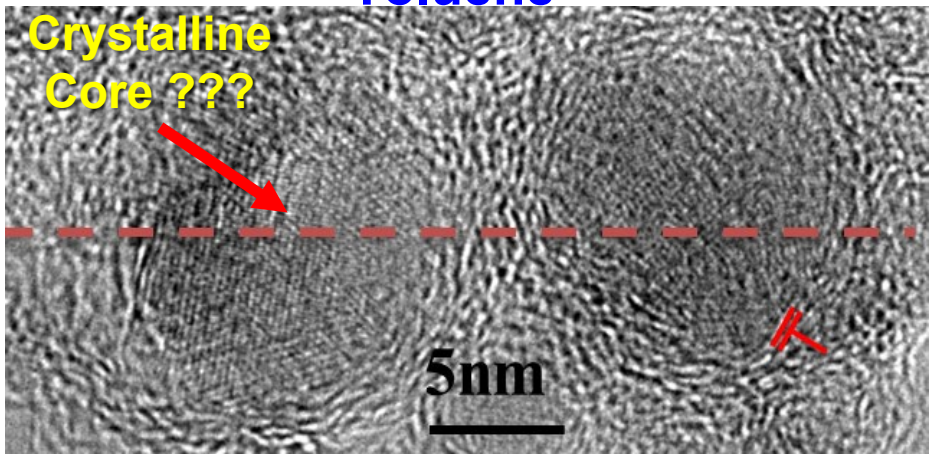

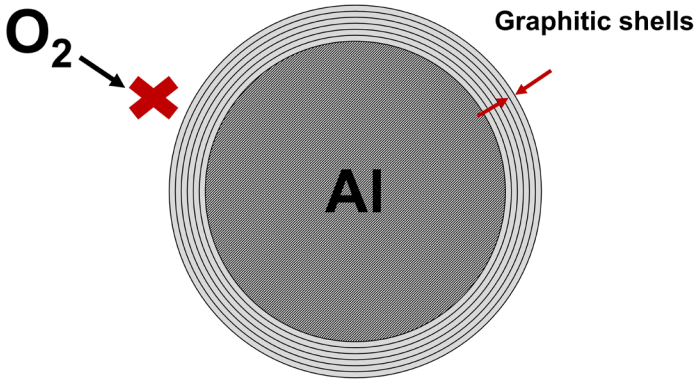

Graphitic shell coated Al NPs: Next Gen ENMs

- **Morphology and Structure:** Electron Energy Loss Spectroscopy (EELS)

D_p ~ 45 nm

Acetone

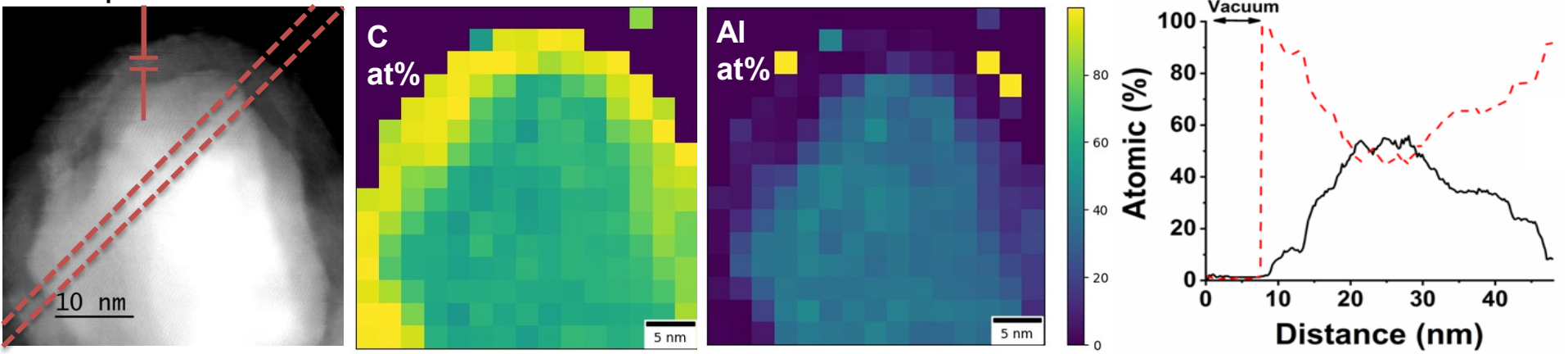

D_p ~ 15 nm

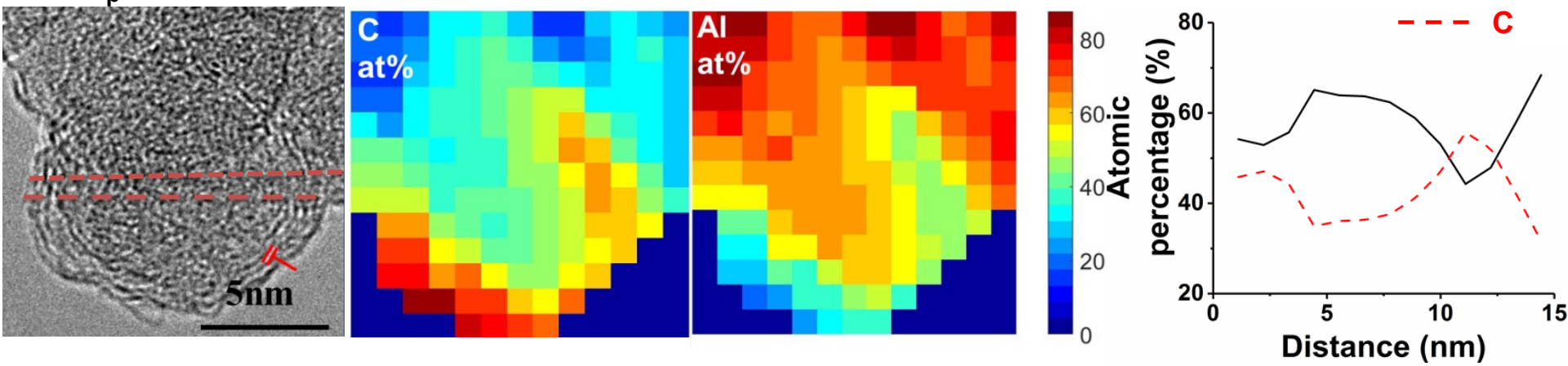

S. A. Davari, J. L. Gottfried, C. Liu, E. L. Ribeiro, G. Duscher, D. Mukherjee, **Appl. Surf. Sci. , 473 (2019)**

Graphitic shell coated Al NPs: Next Gen ENMs

- **Particle Size Distribution:**

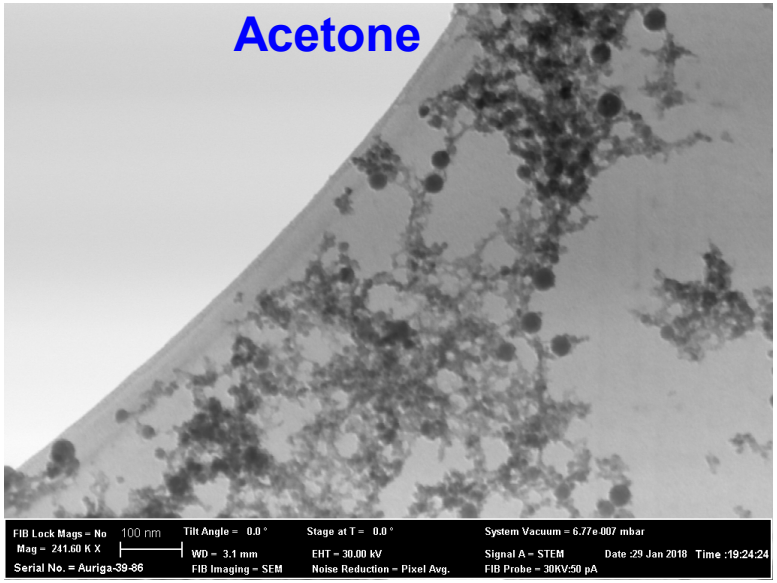

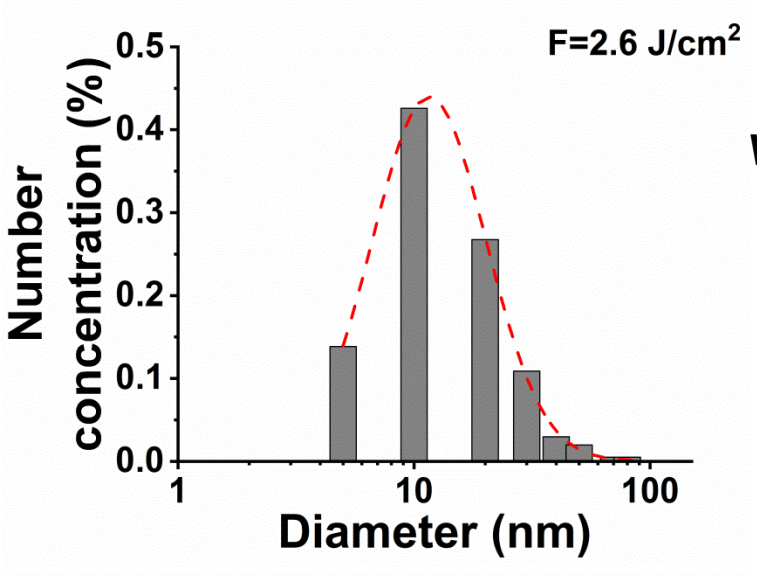

VP_{Acet} ~32 KPa

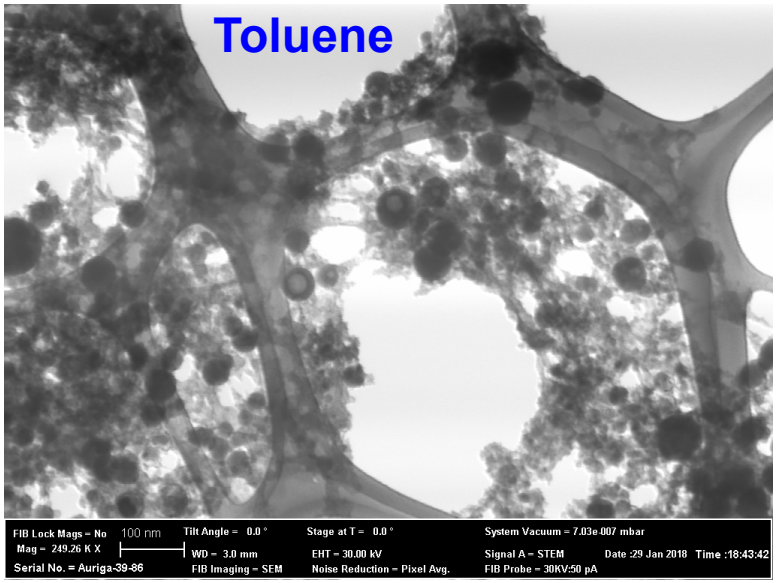

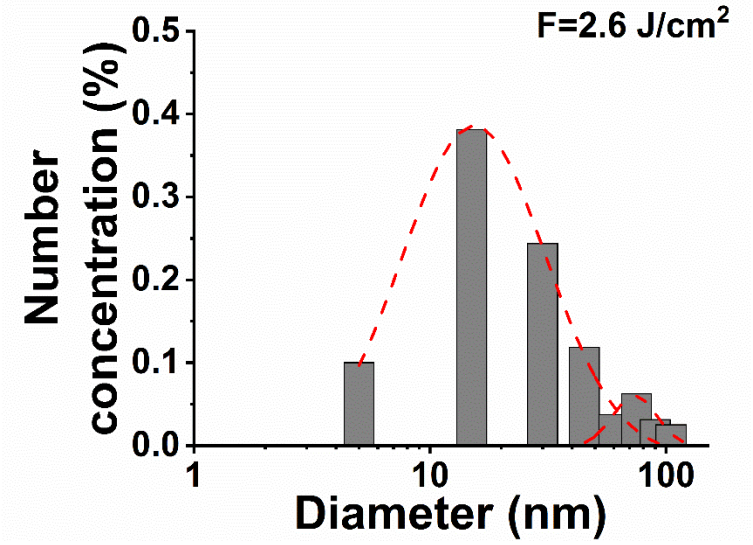

VP_{Tol} ~3.8 KPa

$$r \propto \frac{1}{\ln(S)}$$

S. A. Davari, J. L. Gottfried, C. Liu, E. L. Ribeiro, G. Duscher, D. Mukherjee, **Appl. Surf. Sci. , 473 (2019)**

Graphitic shell coated Al NPs: Next Gen ENMs

- **Energetic Characterization:** **Laser-induced Air Shock from Energetic Materials (LASEM)**

Gottfried J. L., **Propell., Explosives, Pyrotech. (2015)**

U.S. Patent 9,551,692, Issue Date Jan. 24, 2017. ARL docket no. ARL 14-3

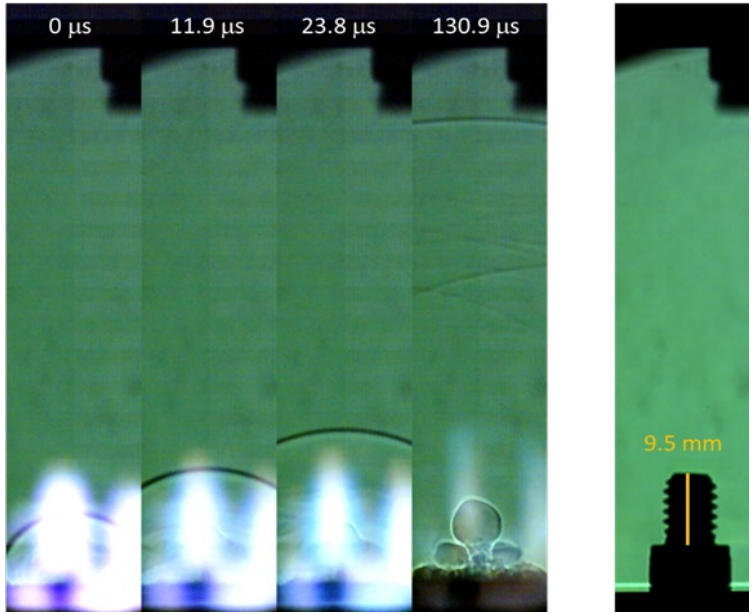

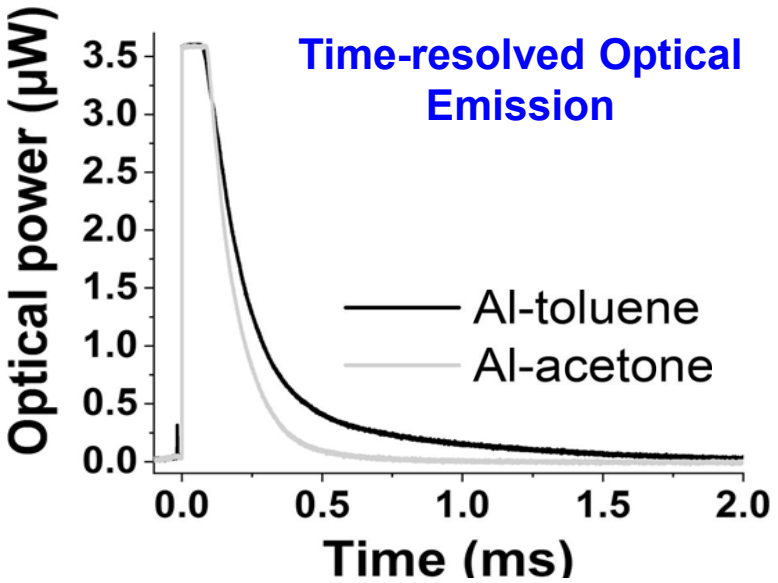

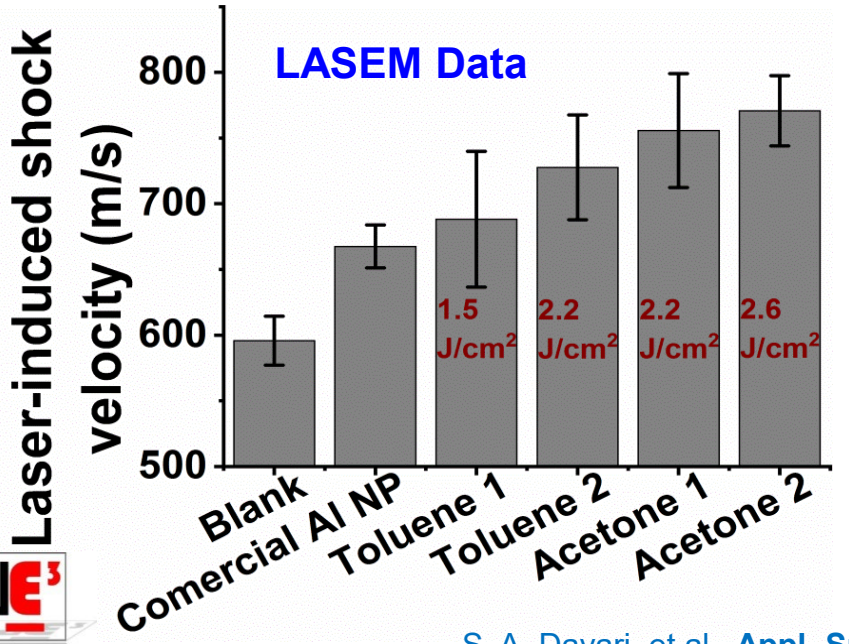

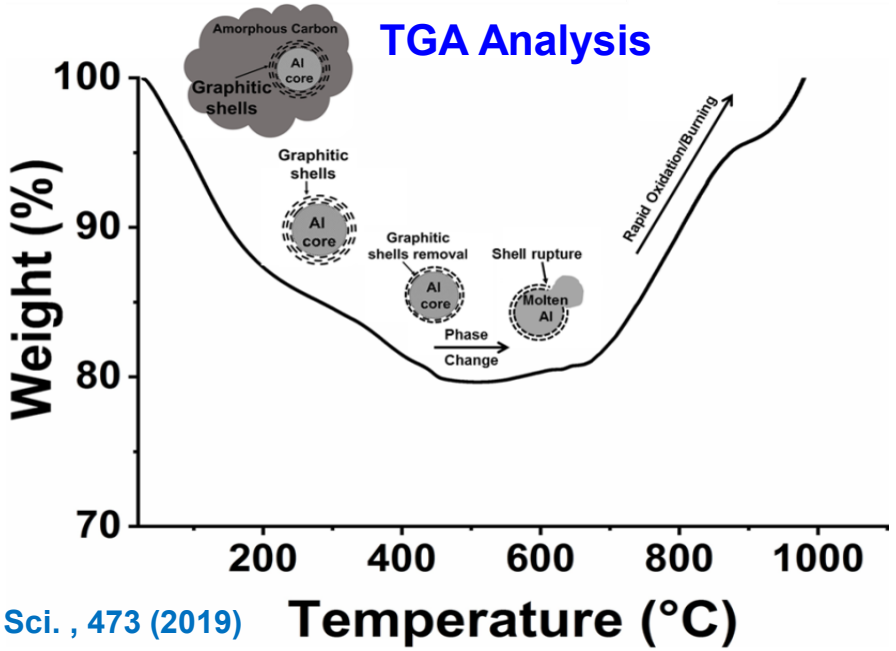

S. A. Davari, et al., **Appl. Surf. Sci. , 473 (2019)**

Graphitic shell coated Al NPs: *Toluene case re-visited!!*

Toluene

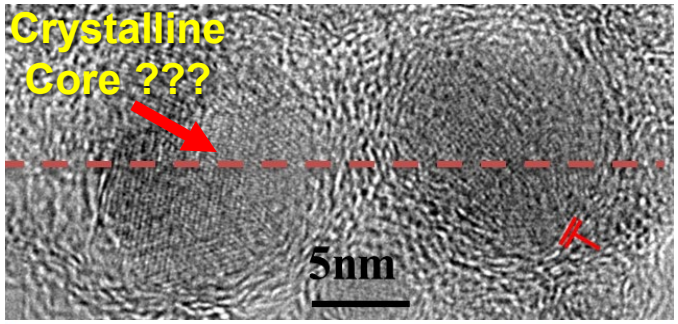

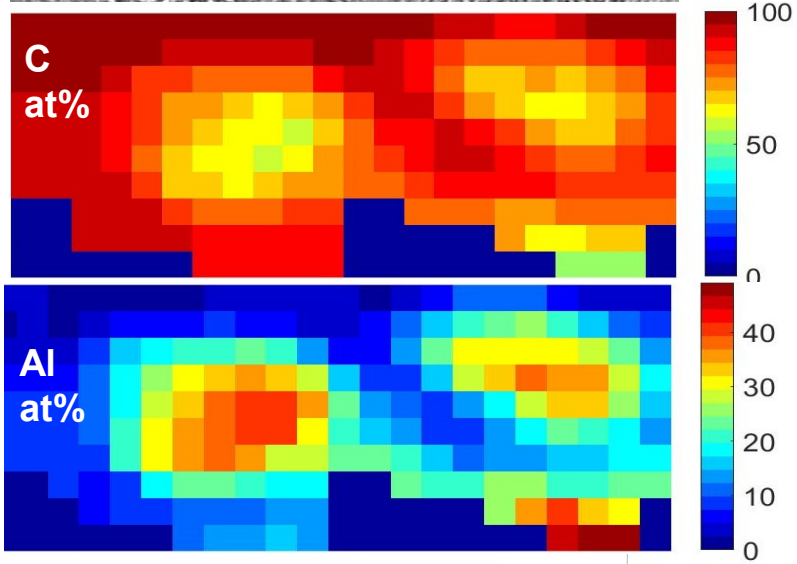

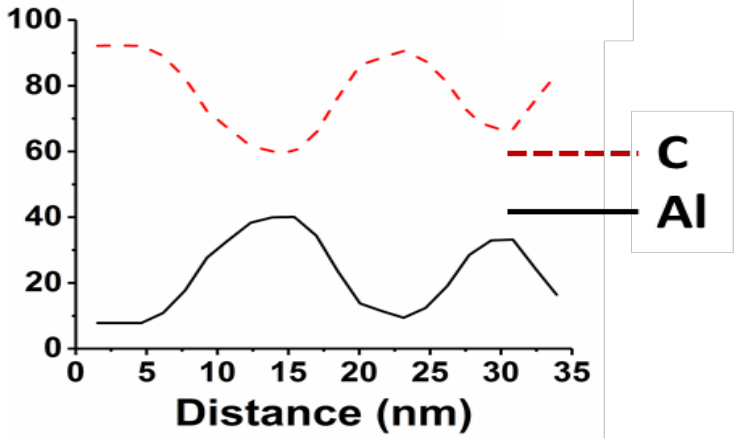

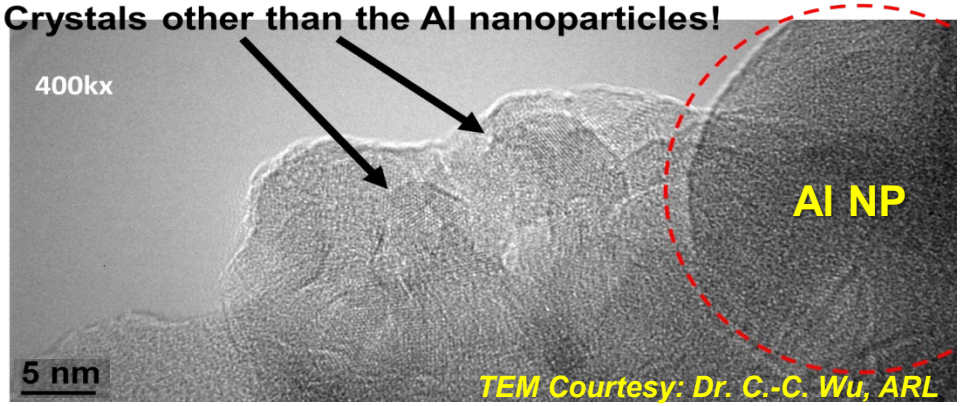

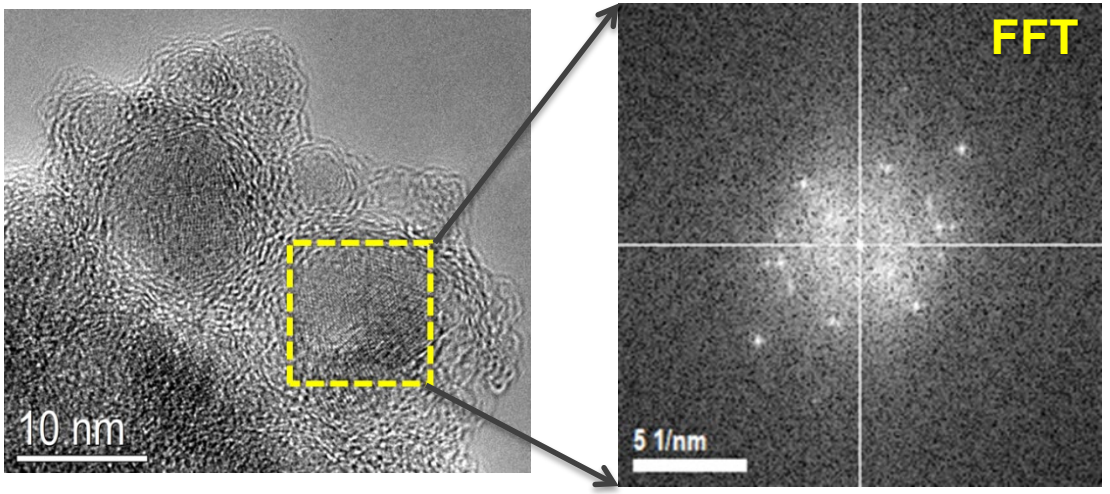

Al_4C_3 [001]: *Rhomohedral with a calculated to be ~* ***0.3335 nm***

Ongoing Investigations:

- Preliminary FFT analysis from HRTEM image reveal crystalline Al_4C_3 structures.
- Detailed XRD & EELS measurements underway to confirm
- Poor resolution due to mixed structures

E. Davis, J. L. Gottfried, G. Duscher, D. Mukherjee, **In Preparation (2019)**

Ongoing Investigation: Preliminary Results

Brief Sample Description List:

High Heat Acetone: *AlC1*

Al target + Acetone in high Press. S.S. chamber
T ~ 90°C; P >> $P_{Saturation\ Vap.}$ to prevent boiling.

Low Laser Flux Acetone: *AlC2*

Al Target + Acetone
P_{atm} ; T_{atm} with low laser flux ~0.5 J/cm^2.

Liquid Nitrogen Acetone: AlC3

Al Target + Acetone in S.S. chamber in liq. N2
T > $T_{freezing}$ (Acetone) ~ -95°C.

High Laser Flux Acetone: *AlC4*

Al Target + Acetone
$P_{atm.}$; T_{atm} with medium laser fluence ~1.00 J/cm^2.

0° C Toluene: *AlC5*

Al Target + Toluene in Al beaker in ice water.
T ~ 0 - 4°C; P_{atm}

For all samples, O_2 was purged from the liquid medium by bubbling compressed N_2.

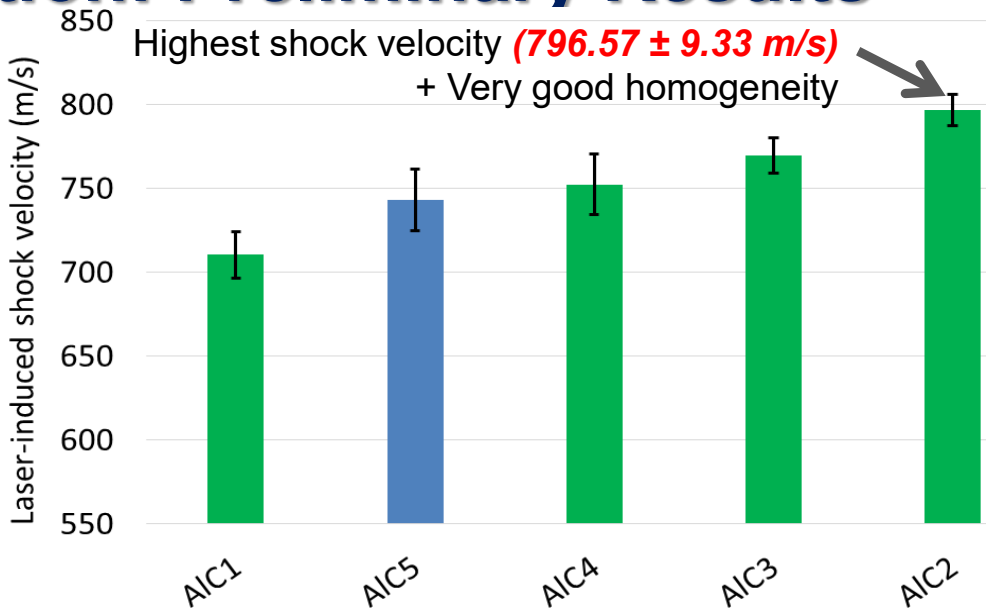

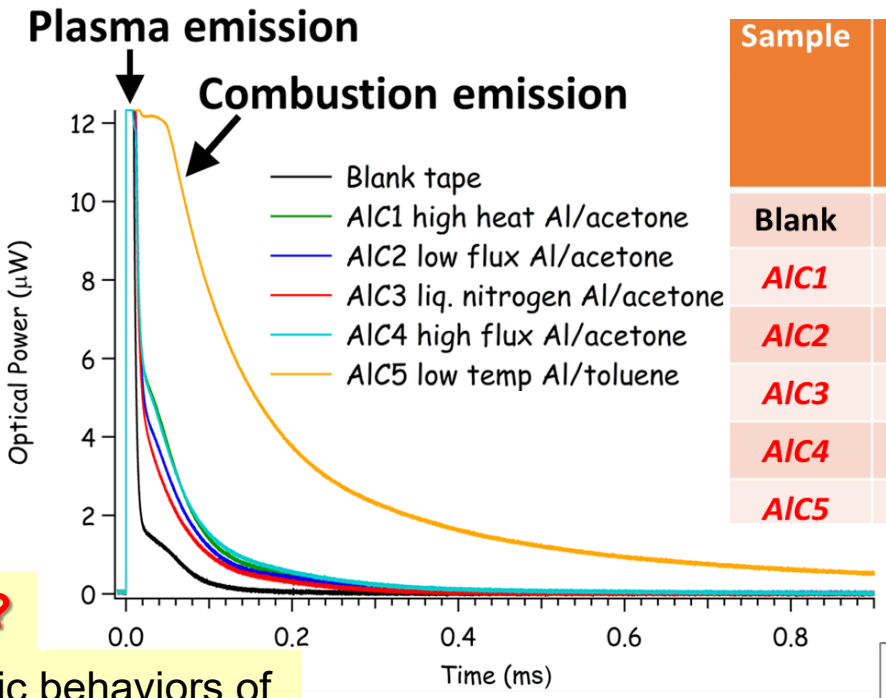

Sample	Integrated combustion emission (mW)
Blank	15.62
AlC1	51.30
AlC2	45.99
AlC3	37.75
AlC4	54.34
AlC5	247.84

An intriguing question??

Mechanistic picture for difference in energetic behaviors of Al/C NP samples prepared in Acetone and Toluene??

E. Davis, et al. **In Preparation (2019)**

Synthesis of composite energetic nanomaterials with tunable interfacial activities via laser ablation synthesis in solution (LASiS)

Graphitic shell coated composite Al/C NPs as energetic nanomaterials (ENMs)

STATUS QUO

➢ **1st Gen Energetic Al NPs: Problems**

- Preserving interfacial activities
- Unwanted oxide shell formation
- Diffusion-limited oxidation
- Excess aggregation

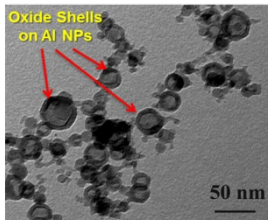

➢ **Existing Challenge:**

Design and facile synthesis of composite ENMs passivated in graphitic shells with kinetically controlled activation

NEW INSIGHTS

- Tunable passivation & activation.
- Stabilization of NPs by C matrix.
- Structure-property relations in composite Al/C ENMs tuned via suitable choice of solvents (Acetone, Toluene), laser fluence and ablations times in LASiS.
- Composition (Al/C/O %wt) & crystalline structures of metastable Al/Al_4C_3 NPs encapsulated in C matrix dictate exothermic/explosive behavior.

MAIN ACHIEVEMENTS:

- Developed chemically clean, facile LASiS technique to synthesize graphitic shell coated composite Al/C NPs in C matrix as superior ENMs.
- Superior performance metrics as compared to commercial energetic Al NPs. Max. laser-induced shock wave velocity **~796.57±9.33 m/s** exceeded desired energetic metrics (>650 m/s).
- ENM size, shape, composition and crystalline structures controlled via solvent and laser parameters.
- Combustion kinetics & thermodynamics tuned via heteronanostructuring of composite Al/C ENMs.

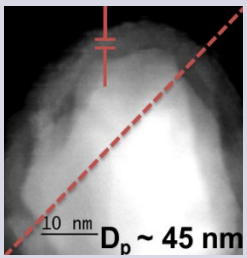

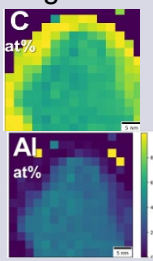

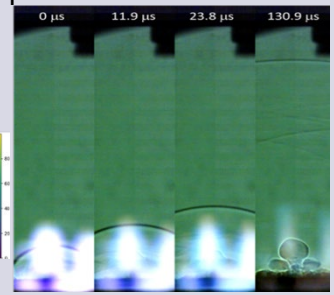

HOW IT WORKS:

- Activation @ 150-200°C burns off C shell/matrix
- Enhances the combustion
- Gaseous by-products (CO_2, CO etc.)
- Graphitic shell hinders coarsening

ASSUMPTIONS AND LIMITATIONS:

- Tailoring accurately the NP compositions (Al/Al_4C_3%wt), interfacial structures and shell thickness.
- Tuning metastable states with Al,C,O ratios to kinetically trap the ENMs.

QUANTITATIVE IMPACT

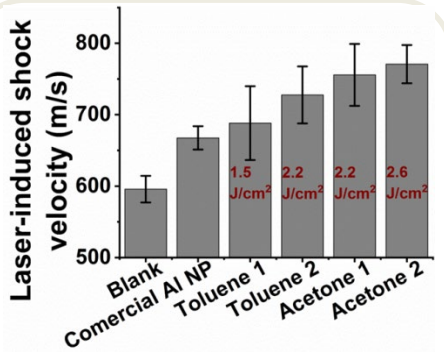

- Max. shock wave velocities from combustion **~796.57±9.33 m/s.**
- Net heat release and kinetics of the ENMs can be tuned via metastable states, compositions and crystalline structures.

END-OF-PHASE GOAL

➢ Tailor accurate composition of Al/C/O ratios for the ENMs.

➢ Ability to tune detonation thermodynamics (*amount of heat release*) and kinetics (*rate of heat release*) by tailoring metastable states and crystalline structures for the composite Al/C ENMs.

➢ Exceed **combustion shock wave velocities > 1000 m/s**

KEY PUBLICATIONS: 1) S. A. Davari et al., *Graphitic coated Al nanoparticles manufactured as superior energetic materials via laser ablation synthesis in organic solvents,* **Appl. Surf. Sci. (2019)**; **2)** S. Hu et al., *Hybrid nanocomposites of nanostructured Co_3O_4 interfaced with reduced/nitrogen-doped graphene oxides for selective improvements in electrocalatytic and/or supercapacitive properties,* **RSC Adv. (2017).**

Acknowledgements

Students:

Seyyed Ali Davari (Graduate, MABE, UTK)
Erick L. Ribeiro (Graduate, CBE, UTK)
Elijah Davis (Graduate, CBE, UTK)
Ravi Pamu (Graduate, MABE, UTK)

Collaborators:

Dr. Jennifer L. Gottfried (US ARL, Aberdeen)
Prof. Gerd Duscher (MSE, UTK)

Thank You !!

Funding:

ARO-STIR
Molecular Structure & Dynamics Program
Program Director: Dr. James Parker

SEERC SUSTAINABLE ENERGY EDUCATION & RESEARCH CENTER

Scientific Support:

ARL U.S. Army Research Lab; Aberdeen, MD

Center for Nanophase Materials Sciences
A Highly Collaborative and Multidisciplinary U.S. DOE Nanoscale Science Research Center

OAK RIDGE NATIONAL LABORATORY
Managed by UT-Battelle for the Department of Energy

Applied Surface Science 473 (2019) 156–163

Contents lists available at ScienceDirect

Applied Surface Science

journal homepage: www.elsevier.com/locate/apsusc

Full Length Article

Graphitic coated Al nanoparticles manufactured as superior energetic materials via laser ablation synthesis in organic solvents

Seyyed Ali Davari[a,b], Jennifer L. Gottfried[c,*], C. Liu[e], Erick L. Ribeiro[d,f], Gerd Duscher[e], Dibyendu Mukherjee[a,d,f,*]

[a] Department of Mechanical, Aerospace, & Biomedical Engineering, University of Tennessee, Knoxville, TN 37996, USA
[b] Department of Mechanical and Aerospace Engineering, Air Quality Research Center (AQRC), University of California Davis, 2132C Bainer Hall, One Shields Ave, Davis, CA 95616, USA
[c] RDRL-WML-B, US Army Research Laboratory, Aberdeen Proving Ground, MD 21005, USA
[d] Department of Chemical & Biomolecular Engineering, University of Tennessee, Knoxville, TN 37996, USA
[e] Department of Material Science and Engineering, University of Tennessee, Knoxville, TN, USA
[f] Nano-BioMaterials Laboratory for Energy, Energetics & Environment (nbml-E^3), University of Tennessee, Knoxville, TN 37996, USA

ARTICLE INFO

Keywords:
Laser ablation synthesis in solution (LASiS)
Organic solvents
Graphitic shell
Aluminum nanoparticles
Energetic nanocomposites

ABSTRACT

The large heat release predicted in the early investigations of energetic aluminum nanoparticles (Al NPs) used in solid-state propulsion and pyrotechnics has been offset by hindered diffusion-limited detonation rates due to excess oxide shell formations and surface area loss from aggregations. We address these challenges by manufacturing graphitic shell coated Al NPs (< 20 nm sizes) via laser ablation synthesis in solution (LASiS) to preserve high surface areas and interfacial properties of Al NPs. Specifically, we use a high-energy laser to ablate Al pellets confined in either acetone or toluene to coat the laser-ablated Al NPs with graphitic shells generated from the thermal pyrolysis of the organic solvents. Energetic activities of the C/Al NPs were tested via the laser-induced air shock from energetic materials (LASEM) technique. We demonstrate that synthesis parameters such as organic solvents, laser flux and ablation times can be tuned to provide superior control of NP sizes/aggregation with the aid of the C shell formations and, in turn, their energetic behavior. This study unveils the synthesis-structure-property relations in LASiS-based manufacturing of energetic nanocapsules within graphitic shells that are safe to handle and can undergo kinetically controlled spontaneous energy release under desired conditions.

1. Introduction

The last few decades have seen a large volume of research work focus on a class of novel metallic materials that demonstrate enhanced energetic properties, thereby finding applications as propellants, explosives and pyrotechnics [1,2]. To this end, past studies involving different mixtures of aluminum (Al) powders and oxidizers as heterogeneous, composite solid propellants have demonstrated high burning rates and enhanced ignition [3–6]. A substantially larger surface area arising from fuel-oxidizer interfaces in the nanoscale regime promotes the kinetically controlled ignition processes. In this regard, the early investigations of energetic nanomaterials primarily focused on the use of metal nanoparticles (NPs), especially nano-Al, in explosives [7–12]. The energetic behavior in these materials is largely driven by the excess interfacial area and small diffusion length scales. In fact, notable works in the past [9,13] have analyzed the unique combustion properties of various energetic materials at nano-scale as compared to their properties at micro-scale. Studies of the heterogeneous combustion characteristics of various nano-powders and nano-composites of explosive materials like ammonium nitrite, cyclotrimethylene trinitramine (RDX), and Al have also been carried out [14]. Such interests have obviously arisen from the increasing need for reliable alternative sources of solid fuel additives and propellants for the ever-expanding and critical defense and aerospace applications.

The combustibility and reactivity of Al particles have been of considerable research interest due to the large negative enthalpy of combustion for Al (e.g., for bulk Al, $\Delta H_B = -1675$ kJ/mol and for a single Al atom, $\Delta H_1 = -2324$ kJ/mol). The difference in enthalpy between bulk and atomic Al has been attributed to the differences in the kinetics of bulk and nanosized particles [2]. Although extensive studies have looked into the gas phase oxidation of micron-sized Al particles in the continuum regime [15], it is obvious from these studies that the criteria

* Corresponding authors at: Department of Mechanical, Aerospace, & Biomedical Engineering, University of Tennessee, Knoxville, TN 37996, USA.
E-mail addresses: jennifer.l.gottfried.civ@mail.mil (J.L. Gottfried), dmukherj@utk.edu (D. Mukherjee).

https://doi.org/10.1016/j.apsusc.2018.11.238
Received 14 September 2018; Received in revised form 21 November 2018; Accepted 29 November 2018
Available online 01 December 2018
0169-4332/

for continuum burning (where particle size is significantly larger than mean free path of the gas) cannot be extended to ultra-fine metal particles (< 100 nm) [12]. Al NP oxidation and its energy release can be described by several mechanisms related to the transport of the participating reactive species and surface reactions, namely: (1) reaction between the background O_2 and the surface Al atoms; (2) formation of oxide layer on the surface Al; (3) diffusion of O_2 and Al through the oxide layer for subsequent reactions. It has been shown that the morphology of the particles, especially the oxide layer thicknesses, changes the energetic properties of Al NPs drastically [16]. The formation of the native oxide layer affects the surface reactivity and oxidation kinetics of Al NPs significantly, as the reaction mechanism proceeds from reaction-limited kinetics at the initial stages on the bare Al surface to a diffusion-limited regime once the reactive species have to diffuse through the pre-formed oxide shell [16]. Therefore, it could be beneficial to design energetic NPs with optimal oxide shells to passivate the Al NP surface for safety reasons, or to tune their surface oxidation rates. Increasing efforts in the design of next-generation energetic nanomaterials have been directed towards the basic idea that the coatings should not simply retard the reactivity, but promote safety while simultaneously enabling performance enhancement. Hence, various scenarios have been suggested to preserve the surface reactivities by using noble metals [17], metal oxides [18] and other potent oxidizers [18–20] to coat the active metal NP. The use of oxidizing agents as the coating on metal NPs also reduces the solid fuel-oxidizer diffusion lengths, thereby promoting the burning rates [21]. Carbon coatings have been demonstrated to show similar features [22], with the added advantage that while the coating itself gets oxidized into gaseous products (CO_2, CO etc.) to prevent any solid ash residues on the particle surface, the Al NP aggregation rates are retarded due to the presence of the carbon shell.

The lab-scale and industrial synthesis of metal NPs typically employ rapid condensation of supersaturated metal vapor (monomers) generated from thermal evaporation of the bulk metal, electric arc discharge, laser ablation, flame reactors, or plasma reactors. Numerous theoretical studies have investigated the formation of Al NPs during gas phase synthesis [23–26]. However, it quickly became apparent that a significant drawback of gas-phase synthesis of metal NPs results from the kinetics of the process, which leads to high particle collision-coalescence rates, rapid aggregation, and loss of interfacial activities. On the other hand, chemical synthesis routes are powerful and have been extensively used to-date. However, they inevitably suffer from harsh residual chemical contaminations and equilibrium growth pathways for the particles, while requiring the use of unwanted surfactants and ligands during the synthesis [27].

Laser ablation techniques are of great interest in synthesis [28–31] and characterization [32–36]. In this regard, laser ablation synthesis in solution (LASiS) has been considered as a “green chemistry” route that does not involve the use of surfactants and harsh reducing agents that typically poison the active surface areas. Previous studies on LASiS [37–45] have extensively developed the technique as a simple, versatile, and chemically clean approach to synthesize wide classes of metal/intermetallic nanoparticles. Moreover, from the industrial perspective, this technique is more economical for facile, rapid and large-scale production as compared to wet chemistry techniques [27]. Our recent series of studies on LASiS has shown that by tuning laser energy, wavelength, target metals of choice, solution chemistry, etc., various nanostructures such as binary nanoalloys, nanocomposites [46–48], ternary nanoalloys [49,50], and 2D materials [51] can be produced with different size, morphology, surface coatings, and chemical compositions. Conventional laser ablation has been employed in the past for the production of bare Al NPs [52]. A few studies have also looked into the size and morphology of Al NPs made from Al target ablation in organic solution [53,54]. Uncertainties in size, morphology, and structure of the Al NPs prevented further development of the technique into reliable and tunable systems that can effectively tailor the surface functionalities and/or coatings on the synthesized NPs. In fact, a vast majority of these studies have largely focused on the mere synthesis of these materials, and are devoid of any comprehensive investigations into tuning the energetic and other surface functional activities of these materials through systematic coatings to preserve solid Al fuel cores and prevent them from unwanted surface oxidation.

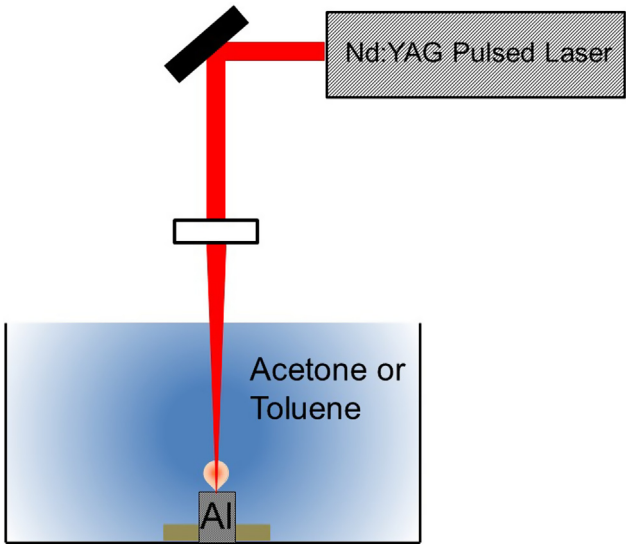

Fig. 1. Schematic for the in-house developed LASiS set-up.

In this paper, we present a facile yet rapid route to synthesize Al NPs with carbon/graphitic coatings as energetic nanomaterials by using LASiS with different organic solvents (acetone, toluene) and laser properties. The size/morphology, interfacial structures, and compositions of the shell-core C/Al NPs have been analyzed in light of their energetic performance as compared to various samples made under different experimental conditions, as well as with commercial native oxide-shell coated nanometer-sized Al powders.

2. Experimental procedure

2.1. LASiS set-up

The LASiS experimental set-up is illustrated in Fig. 1. A Q-switched Nd-YAG pulsed laser operating at 1064 nm with 4 ns pulse width, 10 Hz repetition rate and maximum energy 330 mJ/pulse is used for ablating the target in the cell. The cell is provided with two side-viewing windows to monitor and adjust the laser focal point. A gas inlet and an outlet on the cell allows for suitable purging with inert gases if needed. The Al target is mounted on a stepper motor and rotates continuously to enable uniform ablation from the surface. The reactor cell is also equipped with heating rods, a thermocouple for accurate monitoring of solution temperature, and a sonic dismembrator for in-situ de-agglomeration of the synthesized NPs.

2.2. Synthesis of Al NPs

The Al pellet was purchased from Kurt J. Lesker (99.99% purity, 1″ diameter and 1/4″ height). Two different organic solvents from Sigma-Aldrich (acetone, 99.95% purity and toluene, 99.9% purity) were used in this study for ablation of Al in solution. The Al target was placed in ~8 ml of the organic solvent and ablated with the laser at room temperature. Following laser ablation, the NP suspensions in the organic solvents were centrifuged, decanted and washed with methanol prior to deposition on the TEM grids for imaging, while the dried powder stored under an inert environment was used for all other characterization purposes. Commercial Al NPs (80 nm) were purchased (NovaCentrix) for comparison to the LASiS-synthesized particles.

2.3. Laser-induced air shock from energetic materials (LASEM)

Recently a new technique for measuring the microsecond-timescale energy release of residue materials, laser-induced air shock from energetic materials (LASEM), has been developed in order to estimate the energetic properties of exothermic and explosive materials [55–57]. Briefly, a shock wave is generated in the air above the sample using a focused Nd:YAG laser pulse (1064 nm, 6-ns, 850 mJ) to create a laser-induced plasma on the sample surface. Schlieren imaging with a high-speed camera is subsequently used to track the expansion of the laser-induced shock wave; the measured velocity of the laser-induced shock wave is indicative of the extent of the energy release on the microsecond timescale. For conventional military explosives, a strong correlation between the characteristic laser-induced shock velocity of the material and the measured detonation velocities from large-scale testing was observed. In this work, all LASEM analyses for the as-synthesized and commercial NPs have been carried out at the U.S. Army Research Laboratory facilities. The LASEM samples were prepared by spreading the dry powder in a thin residue affixed to double-sided tape. Excess material not embedded in the tape was ejected away from the sample surface by the laser-induced shock wave and did not chemically react in the laser-induced plasma.

3. Results and discussion

3.1. Structural characterization

Fig. 2 illustrates the STEM images for the NPs generated from the ablation of the Al pellets for 4 min under either acetone or toluene at a laser fluence of 2.6 J/cm^2; HRTEM images for individual particles prepared in acetone or toluene are also shown. For both solvents, the LASiS-synthesized samples consist of Al NPs embedded in a carbon matrix. Fig. 3 illustrates the Raman spectra for samples prepared in either acetone or toluene. It shows that both samples include the D (defect) and G (graphitic) bands at ~1375 and 1585 cm^{-1}, respectively. The observation of D and G bands suggest the presence of amorphous carbon and graphitic structures in both samples. It is noted

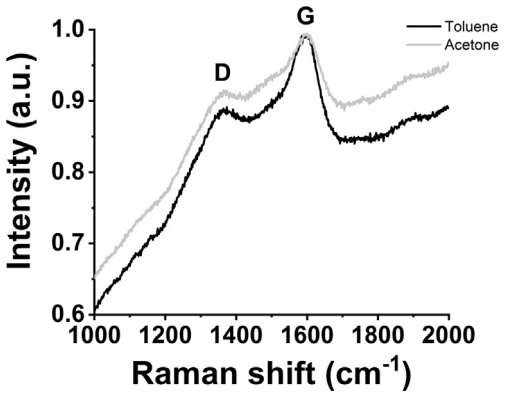

Fig. 3. Raman spectra for the samples prepared in acetone or toluene; labels indicate the well-known D and G bands for carbon.

that the presence of D band stems from the incomplete formation of graphitic shells and/or the amorphous carbon matrix shown in Fig. 2. For detailed investigation of the interfacial structures of the as-produced C/Al composite NPs, electron energy loss spectroscopy (EELS) has been used to analyze the morphology of the particles (Fig. 4). Here, it can be observed that for the synthesis in acetone, the Al NP has been covered with a graphitic shell coating. Moreover, the elemental distribution analysis across the dotted line shown in Fig. 4d confirms the core-shell structure by revealing a carbon-rich shell and central Al core. EELS measurements (shown in Supplementary Information, Fig. S1) for the samples prepared in toluene also revealed nanostructures consisting of Al cores with graphitic shells, although the cores were more crystalline than the samples produced in acetone. Current investigations are underway in our group to further elucidate the detailed structure-composition analysis of the core-shell nanostructures synthesized under different organic solvents.

Supplementary data associated with this article can be found, in the online version, at https://doi.org/10.1016/j.apsusc.2018.11.238.

By comparing Fig. 2a and b, one can immediately observe that the ablation in toluene resulted in larger particles as compared to the

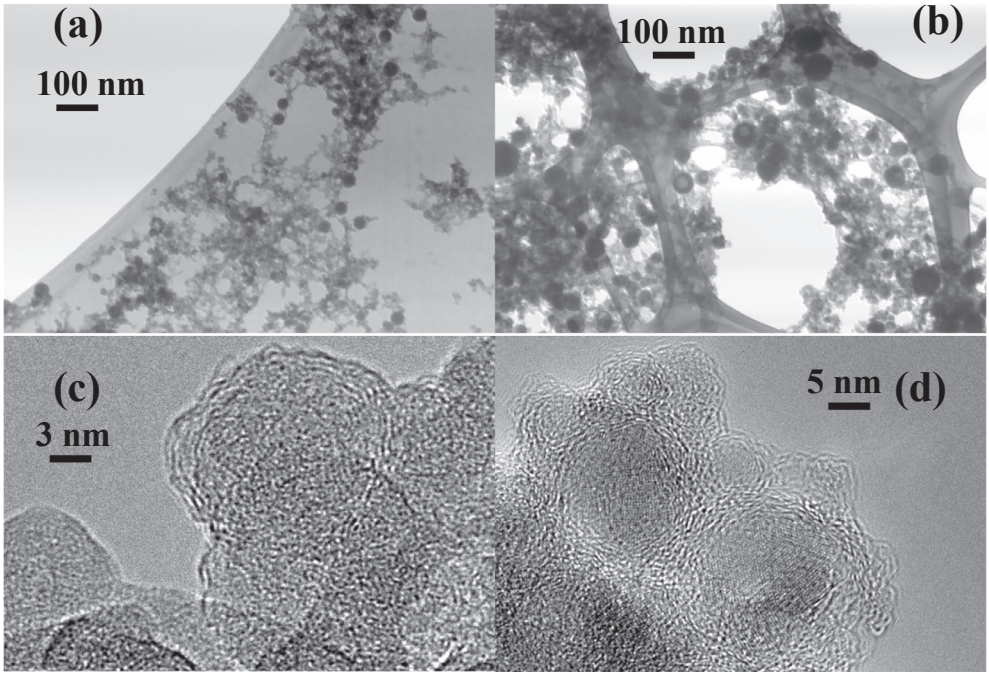

Fig. 2. Scanning transmission electron microscope (STEM) images of composite C/Al NP samples prepared via LASiS in (a) acetone and (b) toluene. High-resolution transmission electron microscope (HRTEM) images of composite C/Al NP samples prepared via LASiS in (c) acetone and (d) toluene.

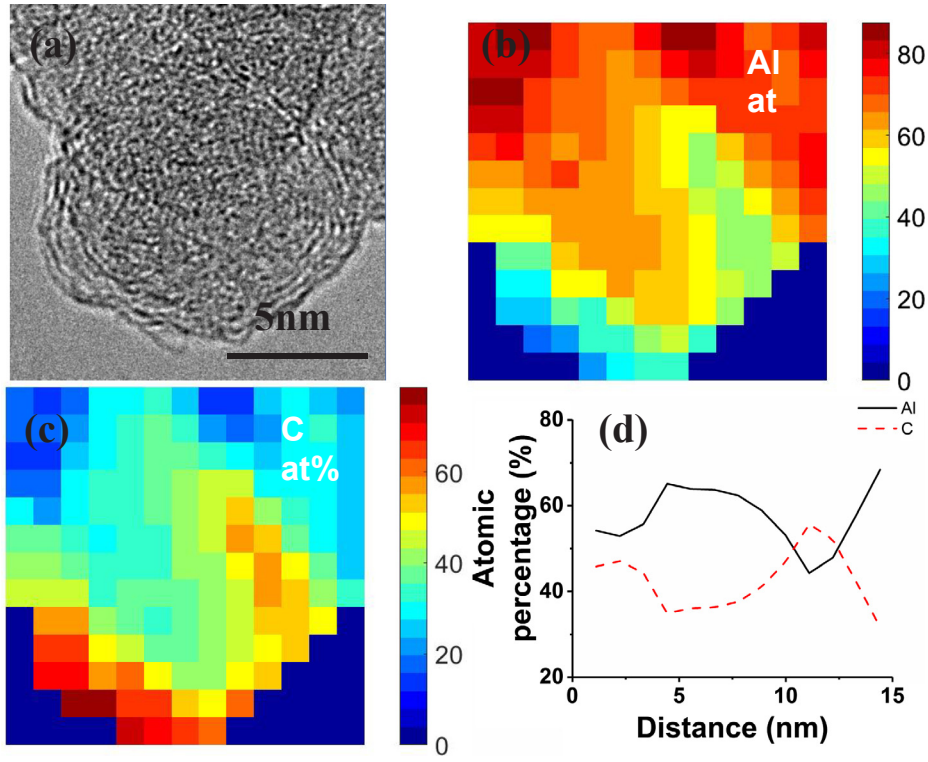

Fig. 4. (a) HRTEM image of the Al/C composite prepared in acetone indicating graphitic shell coatings on the Al NP core. EELS elemental mapping for the corresponding species (b) Al or (c) C. The atomic ratio (%) distributions for Al (solid black line) and C (dashed red line) across the line scan are shown in (d).

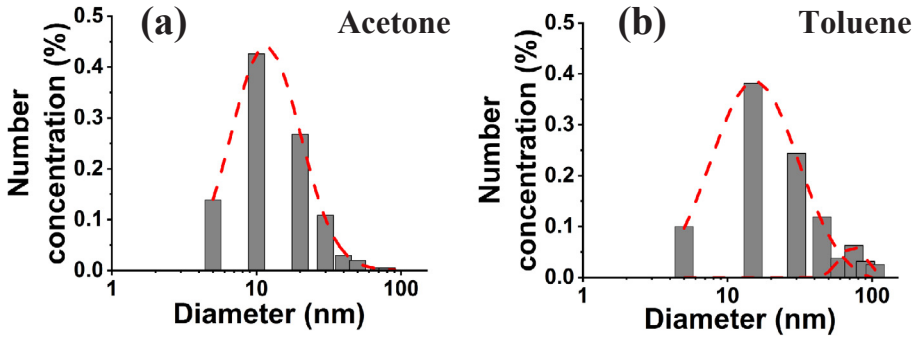

Fig. 5. Effect of organic solvents on the size distributions of the C/Al NPs prepared in (a) acetone and (b) toluene for ablation at a laser fluence of 2.6 J/cm^2 for 4 min.

samples from the ablation in acetone. To confirm these visual observations, the particle size distributions for both cases were analyzed. Fig. 5 shows the size distribution of the particles synthesized in acetone and toluene at a laser fluence of 2.6 J/cm^2 for 4 min. Both samples indicate a lognormal distribution. Based on the size distribution, it can be observed that the samples synthesized in acetone show a unimodal distribution with the peak value at 15.7 nm (log-normal standard deviation of σ = 11.0 nm). On the other hand, the samples synthesized in toluene indicate a bimodal distribution with a major peak at 25 nm (σ = 25.3 nm) and a minor one at 77.2 nm (σ = 17.2 nm). These results could be explained in relation to the distinct vapor pressure (V.P.) differences between acetone (V.P. ~32 kPa) and toluene (V.P. ~3.8 kPa). Particle growth is governed by the nucleation of Al monomers in the plasma-cavitation bubble, which leads to the formation of the primary particles. In general, these primary particles are released into the solution once the cavitation bubble collapses [27,58,59]; they then experience further growth due to coagulation and Al-Al collisions. However, the presence of amorphous carbon produced by the pyrolysis of organic solvents retards the collisions between Al particles and, subsequently, further growth of the Al nanoparticles. Since the vapor pressure of acetone is ~1 order of magnitude greater than toluene, more carbon will be produced due to pyrolysis of organic solvent. Hence, from a simple reaction kinetics analysis where the number of collisions between C and Al particles $N_{carbon-Al} = k_{carbon-Al} n_c n_{Al}$ such that $k_{carbon\text{-}Al}$ is the free molecular collision kernel for the C and Al monomer concentrations n_c and n_{Al}, respectively, $N_{carbon\text{-}Al}$ will be greater in acetone as compared to toluene (i.e., n_c will be larger for acetone). This proposed route of retardation in Al aggregation due to enhanced pyrolysis is also supported by the smaller particle sizes as well as the lower standard deviation in the particle size distribution obtained from acetone.

The effect of ablation time on the particles size distribution has been investigated for the samples in toluene. Fig. 6 shows the particle size distributions obtained for the Al pellets ablated in toluene for 2, 4, 6, and 8 mins at 2 J/cm^2 laser fluence. Here, the size distribution shows a bimodal behavior. As the laser ablation time increases from 2 min to 8 min, the first peak becomes wider (σ = 10.7 nm for 2 min and σ = 18.1 nm for 8 min). Moreover, the second peak at 2 min (~77 nm) shifts to smaller particles at 8 min (~25 nm) as its intensity correspondingly increases. The observation indicates that as the ablation

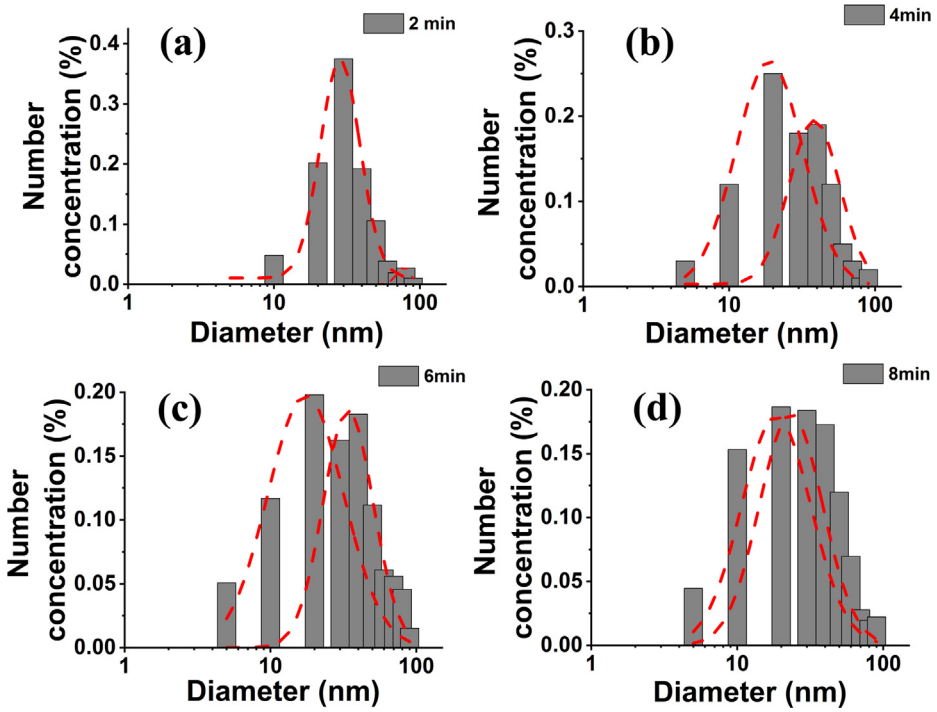

Fig. 6. Effect of laser ablation time on size distribution of the C/Al NPs prepared from LASiS in toluene at 2 J/cm laser fluence.

time increases, the difference between the first and second peaks in terms of the modal size and concentration decreases. Upon considering the free molecular collision kernel for the suspended particles in the solution: $k_{particles}\sqrt{T_{Solution}}$, where $T_{solution}$ represents the solution temperature, one can easily observe that the particle size distribution evolution as a function of the ablation time can be explained by the increase in the solvent temperature and thermal stresses which, in turn, promote aggregation and sintering of the particles.

Further investigations have been carried out on the effect of laser fluence on the particles size distributions. Fig. 7 illustrates the particle size distributions from Al targets ablated in acetone and toluene at 2.6 and 10.5 J/cm^2 laser influences for 4 min. In both the cases, one observes that as the laser fluence increases, the NP modal sizes and the standard deviations become smaller. In the case of acetone, the distribution peak of 15.7 nm (σ = 11.0 nm) at the laser influence of 2.6 J/cm^2 reduces to 12.3 nm (σ = 6.3 nm) at 10.5 J/cm^2. The same results can be seen in toluene wherein a bimodal distribution with peak sizes at 77.2 nm (σ = 17.2 nm) and 25 nm (σ = 25.3 nm) at the laser fluence of 2.6 J/cm^2 shifts to a unimodal distribution with peak size at 17.0 nm (σ = 10.9 nm) for the laser fluence of 10.5 J/cm^2. These results are also

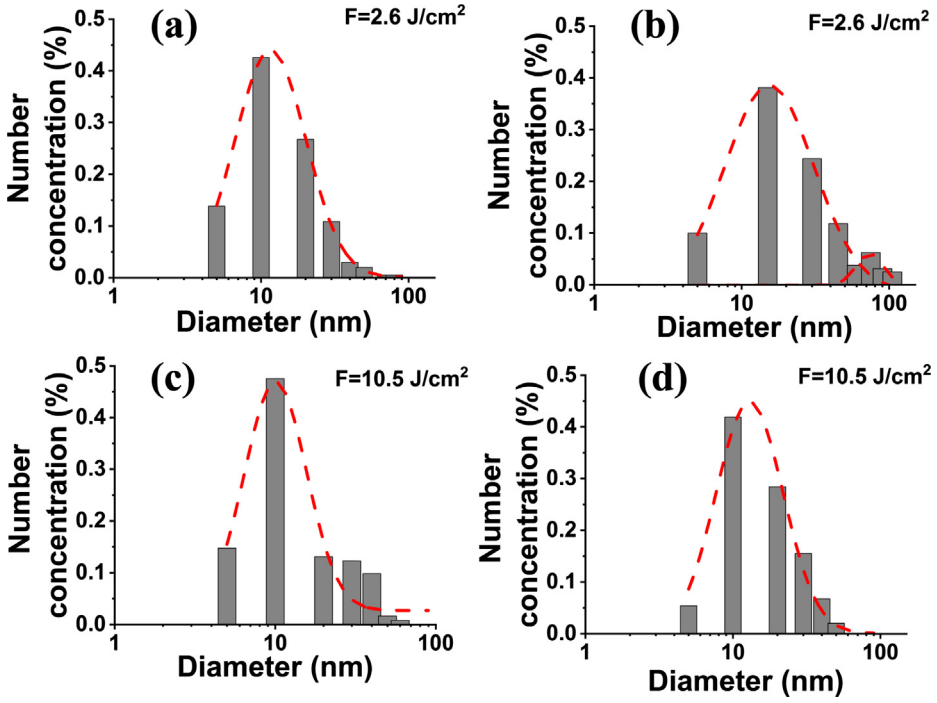

Fig. 7. Effect of laser fluence (F, J/cm^2) on the size distribution of C/Al NPs prepared via LASiS in (a & c) acetone and (b & d) in toluene.

in agreement with previous studies from our group on cobalt nanostructures [60]. The systematic decrease in the particles size can be explained based on the nucleation and formation of primary Al NPs. As the laser fluence increases more Al is ablated, which results in greater Al monomer concentration (n_{Al}). The saturation ratio (S) of Al monomers that encounter gas phase synthesis inside the cavitation bubble is defined as: $S = n_{Al}/n_s$, where n_{Al} is the Al monomer concentration and n_s is the saturated monomer concentration. Therefore, the volume loading and S of Al monomers increase as n_{Al} increases. According to classical nucleation theory (CNT) [61,62], the size of the nucleated primary particles (d^*) is proportional to the inverse of saturation ratio logarithm:

$$d^* = \frac{2\theta}{3\ln(S)}\left(\frac{6v_1}{\pi}\right)^{1/3}$$

where θ is the normalized surface tension of the Al particles and v_1 is the volume of Al monomer. Hence, the increase in the laser fluence results greater saturation ratio and consequently leads to smaller primary particles.

3.2. Energetic characterization

For analyzing the energetic properties of the aforementioned C/Al NP composites, four samples were prepared by ablating the Al target for 4 min under various laser fluxes in acetone or toluene and tested using LASEM. Fig. 8 illustrates the laser-induced shock velocities measured for these samples, as compared to commercial nano-sized energetic Al powders with a native oxide layer. The blank indicates the laser-induced shock velocity for the inert substrate (double-sided tape). Comparing the LASEM results for the laser-induced shock velocities (m/s) from blank substrate (control) to the Al samples, one can immediately notice the increase in the velocities for the Al-containing particles as a result of fast exothermic reactions on the microsecond timescale. The increase in laser-induced plasma temperature due to the exothermic reactions between Al powder and oxygen (either from the sample or air entrained in the plasma) has been previously observed [63]. The current results confirm the ability of the LASEM technique to detect exothermic energetic behavior via laser-induced shock velocity increases from known metal-based energetic material analytes

Moreover, it can be seen that the C/Al NP composites prepared in toluene or acetone show higher characteristic laser-induced shock velocities (> 690 m/s) as compared to the commercial nano-sized Al powder (~670 m/s). In fact the samples prepared in acetone with laser fluences of 2.2 and 2.6 J/cm^2, having peak sizes ~15 nm and relatively narrow size distributions, produce the highest shock velocities (> 755 m/s). One can explain the enhanced energetic behavior

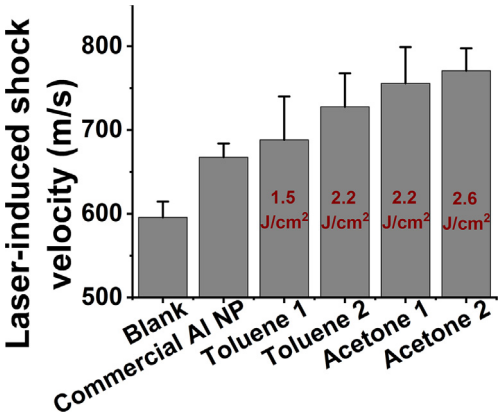

Fig. 8. Comparison of laser-induced shock velocities from LASEM measurements on samples prepared in acetone or toluene at various laser fluences, as compared to commercial nano-Al powders and the blank substrate.

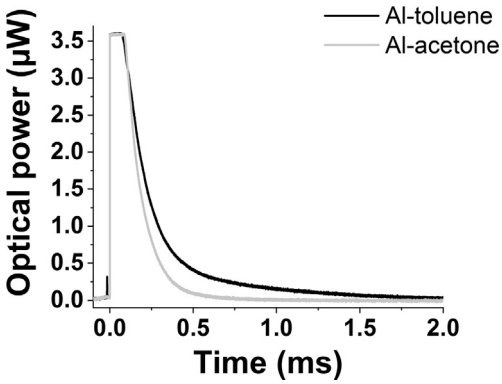

Fig. 9. Time-resolved emission from the reaction of laser-excited C/Al NPs prepared in toluene or acetone.

observed from the synthesized C/Al samples from two perspectives: (1) the protective C/graphitic shells protect the Al NP surfaces from excess oxide layer formation that would hinder the reaction kinetics due to diffusion-limited oxidation pathways through the oxide shell layers; and (2) the earlier onset of pyrolysis in the higher vapor pressure acetone solvent promotes early formation of the amorphous carbon matrix and graphitic structures, dramatically slowing down particle aggregation and thereby generating smaller C/Al NPs (particularly in acetone) which exhibit greater reactivity due to the larger surface area and smaller fuel-oxidizer diffusion length scales. It is well-known from past studies on energetic NPs that as particle sizes decrease, the burning rates and oxidation kinetics become more effective. Here, in the case of the toluene samples, particles show a bimodal size distribution with two modal peaks at 25 nm and 77.2 nm. It is highly likely that the NPs residing at the second peak of 77.2 nm do not undergo complete oxidation on the microsecond-timescale due to the larger sizes and lower surface to volume ratios. Therefore, the bulk of the Al core possibly acts as a dead load during the energy release and retards the energetic reactions. Confirmation of this is the more extensive combustion emission on the millisecond timescale from the C/Al NPs synthesized in toluene (Fig. 9), as compared to the C/Al NPs from acetone that primarily react on the microsecond timescale (as indicated in Fig. 8). While the initial strong emission signal shown in Fig. 9 is a result of the laser-induced plasma emission, combustion of the Al particles following the decay of the plasma appears as a shoulder on this saturated peak. Exothermic reactions that occur later than about 10 μs do not contribute to the laser-induced shock velocity, since at this point in time the shock wave has travelled above the plasma and is only affected by the drag from air.

In a recent study by Gottfried et al. [55], LASEM was effectively employed to correlate laser-induced shock velocity to detonation velocities in order to classify various energetic materials such as TNT (trinitrotoluene), PETN (pentaerythritol trinitrate) etc. as exothermic and/or explosive materials [64]. Upon comparing the LASEM recorded shock velocities from our various C/Al NP composites prepared in toluene and acetone with the known energetic data from the aforesaid study as a function of denotation velocities [64], the C/Al NPs synthesized in toluene clearly indicate exothermic rather than explosive behavior, whereas the samples prepared in acetone fall into the explosive range. However, LASEM estimates of detonation performance assume the material is detonable, and it is not clear how the laser-induced shock velocities of pure metallic samples would correlate to the detonation velocities of organic military explosives [65].

3.3. Oxidative behavior of C/Al NPs: The mechanistic picture

For further investigation into the mechanistic picture behind the excess burning process for the LASiS-synthesized C/Al NPs, Fig. 10 shows the thermo-gravimetric analysis (TGA) for the C/Al sample with

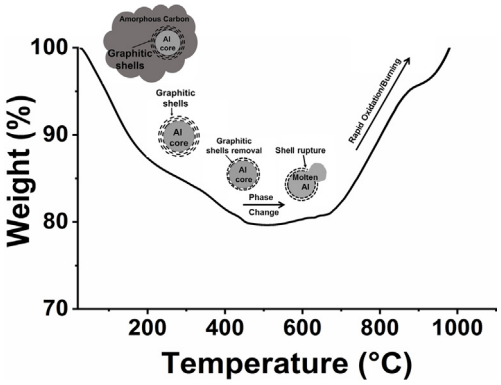

Fig. 10. TGA analysis for the sample with highest LASEM activity (acetone, 2.6 J/cm^2).

the highest LASEM activity (i.e., for samples synthesized in acetone at 2.6 J/cm^2 fluence in Fig. 8). Fig. 10 illustrates thermal decomposition/combustion of the sample in air, by plotting weight as a function of temperature (^{o}C). It can be observed that the sample weight decreases continuously up to ~470 °C. This can be readily explained by the fact that as the amorphous carbon matrix/shell burns, it turns to gaseous by-products such as CO and CO_2 and the sample weight decreases. Between ~470 °C up to ~700 °C the weight does not change drastically, possibly due to phase changes from solid to molten Al prior to the onset of Al oxidation. As also discussed and explained in earlier works for oxide coated Al NPs [66], here the core Al NP melts inside the C shell to generate excess internal pressure due to the large volume expansion which, in turn, ruptures the C shell with relatively lower thermal expansion coefficients. This mechanical rupture releases the highly active and hot molten Al to the oxidizing environment resulting in instantaneous burning/oxidation. Here, one needs to bear in mind that the low young's modulus (~4–30 GPa), high melting point (~3500 °C), and thermal conductivity (~10–114 W/m-K) of graphitic shells play a critical role in heating the encapsulated Al core to its melting point, producing large internal stresses without buckling the shell. Upon reaching a critical activation T and P, such scaffolds typically collapse via melt dispersion or nanoexplosions [67,68] to initiate instantaneous kinetically-driven oxidation of the as-released core nanoclusters. It should be noted that size-dependent Laplace pressure (~surface tension/particle radius) and stress inside such NPs can exceed ambient pressure by many orders of magnitude (~10–20 GPa) [69]. Thus, in the TGA data in Fig. 10, we observe a sudden increase in the sample weight at around ~700 °C. This behavior can be explained by rupture of the remaining graphitic shells between ~470–700 °C and Al oxidation initiation ~700 °C, which consequently increases the sample weight. Previous mass spectrometry studies have also recorded the onset of Al NP oxidation at ~600–700 °C for particle sizes < 50 nm [12]. Added to this, one also needs to bear in mind that while internal pressures inside the shell can rise dramatically for smaller NPs (Laplace pressure effects ~ surface tension/radius) [70], melting points can drop drastically (Tolman effects) [71] – accelerating the phase transition of the Al. In summary, these results are in good agreement with previous studies that have captured similar behavior and temperatures for the oxidation of coated Al NPs [22].

4. Conclusion

LASiS has been employed for synthesizing energetic nanocomposites consisting of graphitic shell coated Al NPs embedded in a carbon matrix. The shell-core C/Al NPs have been prepared through laser ablation in acetone or toluene under various laser fluences. STEM and EELS measurements revealed the size distribution and morphology of the composite C/Al NPs, including the graphitic shell coatings on the Al NP cores. Our results indicate that the size distributions and energetic behavior of the C/Al NPs could be tailored by tuning the LASiS medium (i.e., organic solvent), laser flux and ablation times. The energetic activities of the samples have been tested and compared to a commercial nano-Al powder using LASEM. The results indicate that the samples prepared in acetone or toluene show higher energetic activities as compared to commercial nano-Al powder owing to their smaller sizes and the protective graphitic shell coatings on the Al NPs. Specifically, the C/Al NPs prepared in acetone exhibited higher laser-induced shock velocities as compared to the samples synthesized in toluene, with the samples made from ablation under a laser fluence of 2.6 J/cm^2 indicating the highest activities. Although the C/Al NPs made via LASiS in toluene behave as exothermic materials when compared to their counterparts grown in acetone that exhibit more explosive properties (i.e., react more rapidly), a definitive conclusion on their exothermic/explosive behaviors would demand further investigation into their structure-property characteristics and reaction propagation mechanisms. In addition, refinement of the synthesis process to produce more homogeneously distributed Al NPs with C shells is part of our ongoing research efforts that could provide additional enhancements in the microsecond-timescale energy release. In summary, our work here paves the path for the future design of energetic metal/intermetallic NPs encapsulated in nanostructured graphitic shell coatings and/or fullerene-like layers that can be tailored via LASiS-based techniques to tune their reactive behaviors for a myriad of defense and solid-state propellant applications.

Acknowledgements

Scientific support for this work was provided through the US Army Research Laboratory's (ARL) External Collaboration Initiative (ECI) Award with Dr Jennifer L. Gottfried at the ARL, Aberdeen Proving Ground (APG), Aberdeen, MD.

References

[1] M. Mench, et al., Comparison of thermal behavior of regular and ultra-fine aluminum powders (Alex) made from plasma explosion process, Combust. Sci. Technol. 135 (1–6) (1998) 269–292.
[2] A. Rai, et al., Understanding the mechanism of aluminium nanoparticle oxidation, Combust. Theor. Model. 10 (5) (2006) 843–859.
[3] M.J. Chiaverini, et al., Instantaneous regression behavior of HTPB solid fuels burning with GOX in a simulated hybrid rocket motor, Int. J. Energetic Mater. Chem. Propulsion 4 (1–6) (1997).
[4] J. Renie, et al., Aluminum particle combustion in composite solid propellants, 18th Joint Propulsion Conference, (1982).
[5] N. Bakhman, A. Belyaev, Y.A. Kondrashkov, Influence of the metal additives onto the burning rate of the model solid rocket propellants, Phys. Combust. Explos. 6 (1970) 93.
[6] H. Ritter, S. Braun, High explosives containing ultrafine aluminum ALEX, Propellants Explos. Pyrotech. 26 (6) (2001) 311–314.
[7] A. Ilyin, et al., Characterization of aluminum powders I. Parameters of reactivity of aluminum powders, Propellants Explos. Pyrotech. 27 (6) (2002) 361–364.
[8] P. Brousseau, C.J. Anderson, Nanometric aluminum in explosives, Propellants Explos. Pyrotech. 27 (5) (2002) 300–306.
[9] V. Weiser, S. Kelzenberg, N. Eisenreich, Influence of the metal particle size on the ignition of energetic materials, Propellants Explos. Pyrotech. 26 (6) (2001) 284–289.
[10] L. Zhou, et al., Time-resolved mass spectrometry of the exothermic reaction between nanoaluminum and metal oxides: the role of oxygen release, J. Phys. Chem. C 114 (33) (2010) 14269–14275.
[11] D. Mukherjee, A. Rai, M.R. Zachariah, Quantitative laser-induced breakdown spectroscopy for aerosols via internal calibration: application to the oxidative coating of aluminum nanoparticles, J. Aerosol Sci. 37 (6) (2006) 677–695.
[12] K. Park, et al., Size-resolved kinetic measurements of aluminum nanoparticle oxidation with single particle mass spectrometry, J. Phys. Chem. B 109 (15) (2005) 7290–7299.
[13] M.L. Pantoya, J.J. Granier, Combustion behavior of highly energetic thermites: nano versus micron composites, Propellants Explos. Pyrotech. 30 (1) (2005) 53–62.
[14] A. Pivkina, et al., Nanomaterials for heterogeneous combustion, Propellants Explos. Pyrotech. 29 (1) (2004) 39–48.
[15] R.A. Yetter, G.A. Risha, S.F. Son, Metal particle combustion and nanotechnology, Proc. Combust. Inst. 32 (2) (2009) 1819–1838.
[16] D. Mukherjee, M. Wang, B. Khomami, Impact of particle morphology on surface oxidation of nanoparticles: a kinetic Monte Carlo based study, Aiche J. 58 (11)

(2012) 3341–3353.
[17] E.L. Dreizin, Metal-based reactive nanomaterials, Prog. Energy Combust. Sci. 35 (2) (2009) 141–167.
[18] A. Prakash, A.V. McCormick, M.R. Zachariah, Tuning the reactivity of energetic nanoparticles by creation of a core-shell nanostructure, Nano Lett. 5 (7) (2005) 1357–1360.
[19] K. Sullivan, G. Young, M.R. Zachariah, Enhanced reactivity of nano-B/Al/CuO MIC's, Combust. Flame 156 (2) (2009) 302–309.
[20] A. Prakash, A.V. McCormick, M.R. Zachariah, Synthesis and reactivity of a super-reactive metastable intermolecular composite formulation of Al/KMnO4, Adv. Mater. 17 (7) (2005) p. 900-+.
[21] R.J. Jouet, et al., Surface passivation of bare aluminum nanoparticles using perfluoroalkyl carboxylic acids, Chem. Mater. 17 (11) (2005) 2987–2996.
[22] K. Park, A. Rai, M. Zachariah, Characterizing the coating and size-resolved oxidative stability of carbon-coated aluminum nanoparticles by single-particle mass-spectrometry, J. Nano. Res. 8 (3–4) (2006) 455–464.
[23] S.A. Davari, D. Mukherjee, Kinetic Monte Carlo simulation for homogeneous nucleation of metal nanoparticles during vapor phase synthesis, AIChE J. 64 (1) (2018) 18–28.
[24] D. Mukherjee, S.A. Davari, Computational modeling for fate, transport and evolution of energetic metal nanoparticles grown via aerosol route, Energetic Materials, Springer, 2017, pp. 271–341.
[25] D. Mukherjee, A. Prakash, M.R. Zachariah, Implementation of a discrete nodal model to probe the effect of size-dependent surface tension on nanoparticle formation and growth, J. Aerosol Sci. 37 (10) (2006) 1388–1399.
[26] A. Prakash, A.P. Bapat, M.R. Zachariah, A simple numerical algorithm and software for solution of nucleation, surface growth, and coagulation problems, Aerosol Sci. Technol. 37 (11) (2003) 892–898.
[27] D. Zhang, B. Gökce, S. Barcikowski, Laser synthesis and processing of colloids: fundamentals and applications, Chem. Rev. 117 (5) (2017) 3990–4103.
[28] A.M. Morales, C.M. Lieber, A laser ablation method for the synthesis of crystalline semiconductor nanowires, Science 279 (5348) (1998) 208–211.
[29] W.S. Shi, et al., Laser ablation synthesis and optical characterization of silicon carbide nanowires, J. Am. Ceram. Soc. 83 (12) (2000) 3228–3230.
[30] G.P. Johnston, et al., Reactive laser ablation synthesis of nanosize alumina powder, J. Am. Ceram. Soc. 75 (12) (1992) 3293–3298.
[31] D.P. Yu, et al., Synthesis of boron nitride nanotubes by means of excimer laser ablation at high temperature, Appl. Phys. Lett. 72 (16) (1998) 1966–1968.
[32] A. Ciucci, et al., New procedure for quantitative elemental analysis by laser-induced plasma spectroscopy, Appl. Spectrosc. 53 (8) (1999) 960–964.
[33] S.A. Davari, et al., Calibration-free quantitative analysis of thin-film oxide layers in semiconductors using laser induced breakdown spectroscopy (LIBS), J. Anal. At. Spectrom. 32 (7) (2017) 1378–1387.
[34] D.W. Hahn, N. Omenetto, Laser-induced breakdown spectroscopy (LIBS), Part II: review of instrumental and methodological approaches to material analysis and applications to different fields, Appl. Spectrosc. 66 (4) (2012) 347–419.
[35] S.A. Davari, et al., In-vitro analysis of early calcification in aortic valvular interstitial cells using Laser-Induced Breakdown Spectroscopy (LIBS), J. Biophoton. (2018) 11(1).
[36] S.A. Davari, et al., Detection of interstitial oxygen contents in Czochralski grown silicon crystals using internal calibration in laser-induced breakdown spectroscopy (LIBS), Talanta 193 (2019) 192–198.
[37] V. Amendola, M. Meneghetti, Laser ablation synthesis in solution and size manipulation of noble metal nanoparticles, PCCP 11 (20) (2009) 3805–3821.
[38] D. Mukherjee, S. Hu, Compositions, Systems and Methods for Producing Nanoalloys, and/or Nanocomposites using tandem Laser Ablation Synthesis in Solution-Galvanic Replacement Reaction, 2016, USA.
[39] D.S. Zhang, B. Goekce, S. Barcikowski, Laser synthesis and processing of colloids: fundamentals and applications, Chem. Rev. 117 (5) (2017) 3990–4103.
[40] A. Letzel, et al., Size quenching during laser synthesis of colloids happens already in the vapor phase of the cavitation bubble, J. Phys. Chem. C 121 (9) (2017) 5356–5365.
[41] M.R. Kalus, et al., How persistent microbubbles shield nanoparticle productivity in laser synthesis of colloids – quantification of their volume, dwell dynamics, and gas composition, PCCP 19 (10) (2017) 7112–7123.
[42] V. Amendola, S. Barcikowski, A quarter-century of nanoparticle generation by lasers in liquids: where are we now, and what's next? J. Colloid Interface Sci. 489 (2017) 1–2.
[43] O. Prymak, et al., Crystallographic characterization of laser-generated, polymer-stabilized 4 nm silver-gold alloyed nanoparticles, Mater. Chem. Phys. 207 (2018) 442–450.
[44] G. Marzun, et al., Role of dissolved and molecular oxygen on Cu and PtCu alloy particle structure during laser ablation synthesis in liquids, ChemPhysChem 18 (9) (2017) 1175–1184.
[45] G. Marzun, et al., Size control and supporting of palladium nanoparticles made by laser ablation in saline solution as a facile route to heterogeneous catalysts, Appl. Surf. Sci. 348 (2015) 75–84.
[46] S. Hu, et al., PtCo/CoOx nanocomposites: bifunctional electrocatalysts for oxygen reduction and evolution reactions synthesized via tandem laser ablation synthesis in solution-galvanic replacement reactions, Appl. Catal. B-Environ. 182 (2016) 286–296.
[47] S.A. Davari, S. Hu, D. Mukherjee, Calibration-free quantitative analysis of elemental ratios in intermetallic nanoalloys and nanocomposites using Laser Induced Breakdown Spectroscopy (LIBS), Talanta 164 (2017) 330–340.
[48] S. Hu, et al., Tandem laser ablation synthesis in solution-galvanic replacement reaction (LASiS-GRR) for the production of PtCo nanoalloys as oxygen reduction electrocatalysts, J. Power Sources 306 (2016) 413–423.
[49] S.A. Davari, et al., Rapid elemental composition analysis of intermetallic ternary nanoalloys using calibration-free quantitative Laser Induced Breakdown Spectroscopy (LIBS), MRS Adv. 2 (55) (2017) 3371–3376.
[50] S. Hu, et al., A facile and surfactant-free route for nanomanufacturing of tailored ternary nanoalloys as superior oxygen reduction reaction electrocatalysts, Catal. Sci. Technol. 7 (10) (2017) 2074–2086.
[51] S. Hu, et al., Hybrid nanocomposites of nanostructured Co3O4 interfaced with reduced/nitrogen-doped graphene oxides for selective improvements in electrocatalytic and/or supercapacitive properties, RSC Adv. 7 (53) (2017) 33166–33176.
[52] A. Baladi, R.S. Mamoory, Investigation of different liquid media and ablation times on pulsed laser ablation synthesis of aluminum nanoparticles, Appl. Surf. Sci. 256 (24) (2010) 7559–7564.
[53] R. Kuladeep, et al., Investigation of optical limiting properties of Aluminium nanoparticles prepared by pulsed laser ablation in different carrier media, J. Appl. Phys. 114 (24) (2013) 243101.
[54] G. Viau, et al., Internal structure of Al hollow nanoparticles generated by laser ablation in liquid ethanol, Chem. Phys. Lett. 501 (4–6) (2011) 419–422.
[55] J.L. Gottfried, Laboratory-scale method for estimating explosive performance from laser-induced shock waves, Propellants Explos. Pyrotech. 40 (5) (2015) 674–681.
[56] J.L. Gottfried, T.M. Klapötke, T.G. Witkowski, Estimated detonation velocities for TKX-50, MAD-X1, BDNAPM, BTNPM, TKX-55, and DAAF using the laser–induced air shock from energetic materials technique, Propellants Explos. Pyrotech. 42 (4) (2017) 353–359.
[57] J.L. Gottfried, E.J. Bukowski, Laser-shocked energetic materials with metal additives: evaluation of chemistry and detonation performance, Appl. Opt. 56 (3) (2017) B47–B57.
[58] S. Ibrahimkutty, et al., Nanoparticle formation in a cavitation bubble after pulsed laser ablation in liquid studied with high time resolution small angle x-ray scattering, Appl. Phys. Lett. 101 (10) (2012) 103104.
[59] J. Lam, et al., γ-Al 2 O 3 nanoparticles synthesised by pulsed laser ablation in liquids: a plasma analysis, PCCP 16 (3) (2014) 963–973.
[60] S. Hu, C. Melton, D. Mukherjee, A facile route for the synthesis of nanostructured oxides and hydroxides of cobalt using laser ablation synthesis in solution (LASIS), PCCP 16 (43) (2014) 24034–24044.
[61] S.L. Girshick, C.P. Chiu, Homogeneous nucleation of particles from the vapor-phase in thermal plasma synthesis, Plasma Chem. Plasma Process. 9 (3) (1989) 355–369.
[62] S.L. Girshick, P. Agarwal, D.G. Truhlar, Homogeneous nucleation with magic numbers: aluminum, J. Chem. Phys. (2009) 131.
[63] J.L. Gottfried, Laser-induced plasma chemistry of the explosive RDX with various metallic nanoparticles, Appl. Opt. 51 (7) (2012) B13–B21.
[64] J.L. Gottfried, Influence of exothermic chemical reactions on laser-induced shock waves, PCCP 16 (39) (2014) 21452–21466.
[65] J.L. Gottfried, et al., Estimating the relative energy content of reactive materials using nanosecond-pulsed laser ablation, MRS Adv. (2018) 1–12.
[66] A. Rai, et al., Importance of phase change of aluminum in oxidation of aluminum nanoparticles, J. Phys. Chem. B 108 (39) (2004) 14793–14795.
[67] L. Sun, et al., Plastic deformation of single nanometer-sized crystals, Phys. Rev. Lett. 101 (15) (2008) 156101.
[68] S.F. Son, Encapsulated nanoscale particles and inclusions in solid propellant ingredients, in: V.E. Zarko, A.A. Gromov (Eds.), Energetic Nanomaterials: Synthesis, Characterizations, and Application, Elsevier, 2016.
[69] H. Wang, et al., In situ oxidation of carbon-encapsulated cobalt nanocapsules creates highly active cobalt oxide catalysts for hydrocarbon combustion, Nat. Commun. 6 (2015) 7181.
[70] T. Hawa, M.R. Zachariah, Internal pressure and surface tension of bare and hydrogen coated silicon nanoparticles, J. Chem. Phys. 121 (18) (2004) 9043–9049.
[71] H.M. Lu, Q. Jiang, Size-dependent surface tension and tolman's length of droplets, Langmuir 21 (2) (2005) 779–781.